Supporting Information

CO_2 uptake potential of cerium(III) triazolates and tetrazolates

Jonas Riedmaier, Cäcilia Maichle-Mössmer and Reiner Anwander*

Institut für Anorganische Chemie, Eberhard Karls Universität Tübingen, Auf der Morgenstelle 18, 72076 Tübingen, Germany.

*Email: reiner.anwander@uni-tuebingen.de

Table of Contents

Crystallographic Data……S2
NMR Spectra……S7
IR Spectra……S19
Thermogravimetric Analysis……S22
Absorption Spectra……S24

Crystallographic Data

Table S1. Crystallographic Data for compounds **2**, **5** and **6**

	2	**5**	**6**
CCDC	2530849	2530848	2530847
formula	$C_{56}H_{57}CeN_{10}O_3$	$C_{25}H_{47}CeN_{12}O$	$C_{31}H_{41}CeN_{12}O$
M_r [g/mol]	1058.23	671.86	737.88
color/shape	block/colourless	block/colourless	needle/colourless
crystal dimensions [mm]	0.200 × 0.187 × 0.130	0.221 × 0.217 × 0.171	0.169 × 0.066 × 0.064
crystal system	monoclinic	monoclinic	monoclinic
space group	$P2_1/n$	$P2_1/n$	$P2_1/c$
a [Å]	11.8280(6)	12.0514(2)	8.3105(5)
b [Å]	19.2224(10)	17.0159(3)	20.9901(12)
c [Å]	22.7962(12)	14.9451(3)	19.3244(11)
α [°]	90	90	90
β [°]	98.3820(10)	101.6430(10)	102.2090(10)
γ [°]	90	90	90
V [Å^3]	5127.6(5)	3001.66(9)	3294.7(3)
Z	4	4	4
T [K]	100(2)	100(2)	100(2)
λ [Å]	0.71073	0.71073	0.71073
ρ_{calcd} [g/cm^3]	1.371	1.487	1.488
μ [mm^{-1}]	0.942	1.557	1.427
F (000)	2180	1338	1508
θ range [°]	2.094–28.281	1.835–30.540	1.450–31.696
unique reflections	12721	9185	10925
total reflections	101090	88171	76123
R_1[a]/wR_2[b] (I>2σ)	0.0275/0.0604	0.0159/0.0390	0.0382/0.0791
R_1[a]/wR_2[b] (all data)	0.0396/0.0669	0.0169/0.0396	0.0633/0.0906
GOF[c]	1.043	1.042	1.038

[a]$R_1 = \Sigma(||F_0| - |F_c||) / \Sigma|F_0|$, $F_0 > 4\sigma(F_0)$, [b]$wR_2 = \{\Sigma[w(F_0^2 - F_c^2)^2 / \Sigma[w(F_0^2)^2]\}^{1/2}$. [c]$GOF = [\Sigma w(F_0^2 - F_c^2)^2 / (n_0 - n_p)]^{1/2}$.

Table S2. Crystallographic Data for compounds **7** and **8**

	7	**8**
CCDC	2530850	2530846
formula	$C_{34}H_{44}CeN_{15}O$	$C_{24}H_{42}CeN_9$
M_r [g/mol]	818.96	596.78
color/shape	block/colourless	block/colourless
crystal dimensions [mm]	0.268 × 0.214 × 0.165	0.204 × 0.127 × 0.121
crystal system	orthorhombic	trigonal
space group	$Pca2_1$	$R3$
a [Å]	23.6496(12)	17.6019(4)
b [Å]	13.5831(7)	17.6019(4)
c [Å]	15.2537(8)	7.6464(3)
α [°]	90	90
β [°]	90	90
γ [°]	90	120
V [Å^3]	4900.0(4)	2051.67(13)
Z	4	3
T [K]	100(2)	100(2)
λ [Å]	0.71073	0.71073
ρ_{calcd} [g/cm^3]	1.110	1.449
μ [mm^{-1}]	0.967	1.693
F (000)	1676	921
θ range [°]	2.179–33.639	2.314–33.582
unique reflections	18808	3436
total reflections	148721	14307
R_1[a]/wR_2[b] (I>2σ)	0.0264/0.0574	0.0168/0.0422
R_1[a]/wR_2[b] (all data)	0.0354/0.0613	0.0168/0.0422
GOF[c]	1.026	1.100

[a]$R_1 = \Sigma(||F_0| - |F_c||) / \Sigma|F_0|$, $F_0 > 4\sigma(F_0)$, [b]$wR_2 = \{\Sigma[w(F_0^2 - F_c^2)^2 / \Sigma[w(F_0^2)^2]\}^{1/2}$. [c]$GOF = [\Sigma w(F_0^2 - F_c^2)^2 / (n_0 - n_p)]^{1/2}$.

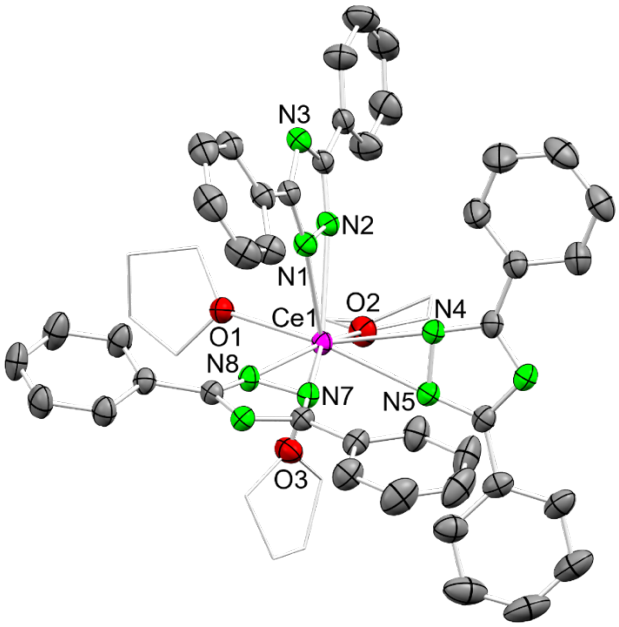

Figure S1. Crystal structure of $Ce(tz^{Ph,Ph})_3(thf)_3$ (**2**). Ellipsoids are shown at a 50% probability level. THF carbon atoms are represented as a wireframe model. Disordered and hydrogen atoms are omitted for clarity. Selected interatomic distances [Å]: Ce1–N1 2.4650(17), Ce1–N2 2.5535(16), Ce1–N4 2.4700(16), Ce1–N5 2.5324(16), Ce1–N7 2.4908(16), Ce1–N8 2.5123(15), Ce1–O1 2.5680(13), Ce1–O2 2.5690(14), Ce1–O3 2.5773(15). Selected angles [°]: N1–Ce1–O3 154.23(5), O1–Ce1–O3 80.90(5).

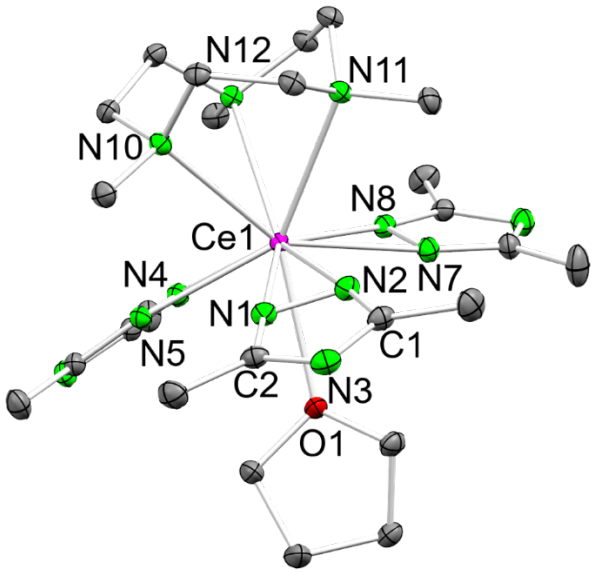

Figure S2. Crystal structure of $(Me_3TACN)Ce(tz^{Me,Me})_3(thf)$ (**5**). Ellipsoids are shown at a 50% probability level. Hydrogen atoms are omitted for clarity. Selected interatomic distances [Å]: Ce1–N1 2.5435(9), Ce1–N2 2.5921(9), Ce1–N4 2.5020(9), Ce1–N5 2.5626(9), Ce1–N7 2.5159(9), Ce1–N8 2.5985(9), Ce1–N10 2.7714(9), Ce1–N11 2.7743(9), Ce1–N12 2.7975(9), Ce1–O1 2.7259(8), N1–N2 1.3866(13), C1–N2 1.3349(14), C1–N3 1.3529(15), C2–N1 1.3332(14), C2–N3 1.3500(15). Selected angles [°]: N10–Ce1–N1 77.23(3), N10–Ce1–N2 92.62(3).

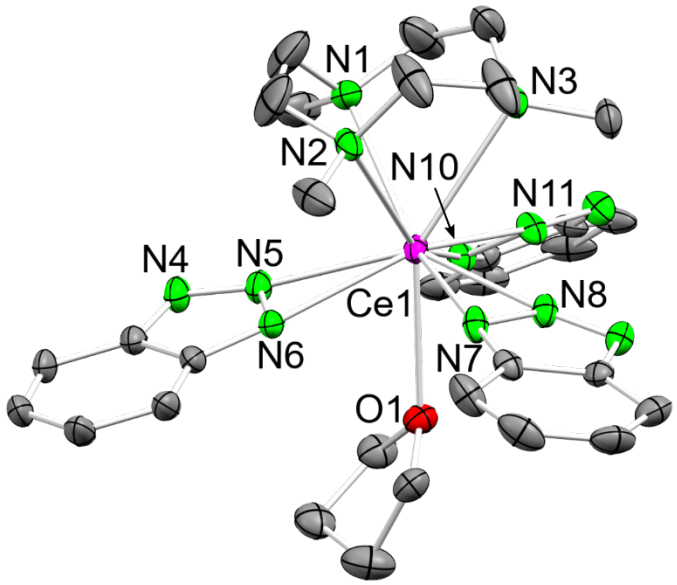

Figure S3. Crystal structure of $(Me_3TACN)Ce(trz^{Bz})_3(thf)$ (**6**). Ellipsoids are shown at a 50% probability level. Disordered and hydrogen atoms are omitted for clarity. Selected interatomic distances [Å]: Ce1–N1 2.733(2), Ce1–N2 2.737(2), Ce1–N3 2.765(2), Ce1–N5 2.536(2), Ce1–N6 2.548(2), Ce1–N7 2.552(2), Ce1–N8 2.529(2), Ce1–O1 2.6693(19). Selected angles [°]: N1–Ce1–N5 75.44(7), N1–Ce1–N6 97.31(7).

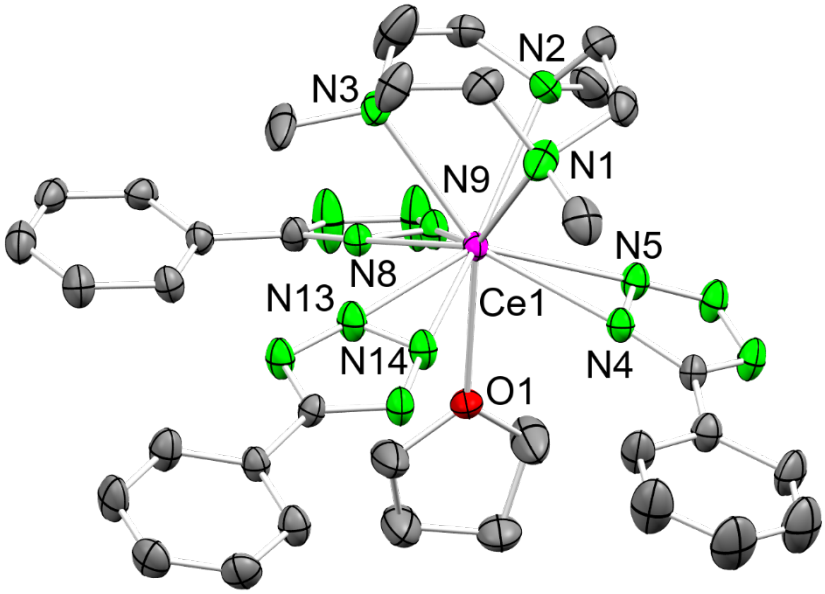

Figure S4. Crystal structure of $(Me_3TACN)Ce(tet^{Ph})_3(thf)$ (**7**). Ellipsoids are shown at a 50% probability level. Disordered and hydrogen atoms are omitted for clarity. Selected interatomic distances [Å]: Ce1–N1 2.722(2), Ce1–N2 2.710(2), Ce1–N3 2.715(2), Ce1–N4 2.5422(19), Ce1–N5 2.595(2), Ce1–N8 2.5482 (19), Ce1–N9 2.587(2), Ce1–N13 2.543(2), Ce1–N14 2.599(2), Ce1–O1 2.6322(18). Selected angles [°]: N1–Ce1–N4 77.57(7), N1–Ce1–N5 89.22(7), N4–Ce1–O1 71.32(6).

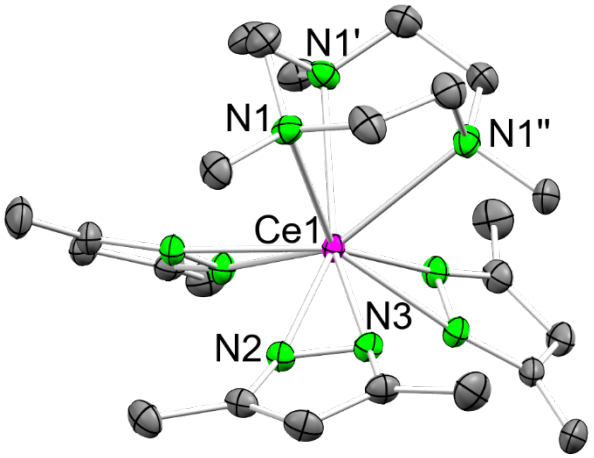

Figure S5. Crystal structure of $(Me_3TACN)Ce(pz^{Me,Me})_3$ (**8**). Ellipsoids are shown at a 50% probability level. Hydrogen atoms are omitted for clarity. Selected interatomic distances [Å]: Ce–N1 2.751(2), Ce1–N2 2.4675(18), Ce1–N3 2.5379(19).

NMR Spectra

Solvent signals are marked with an *

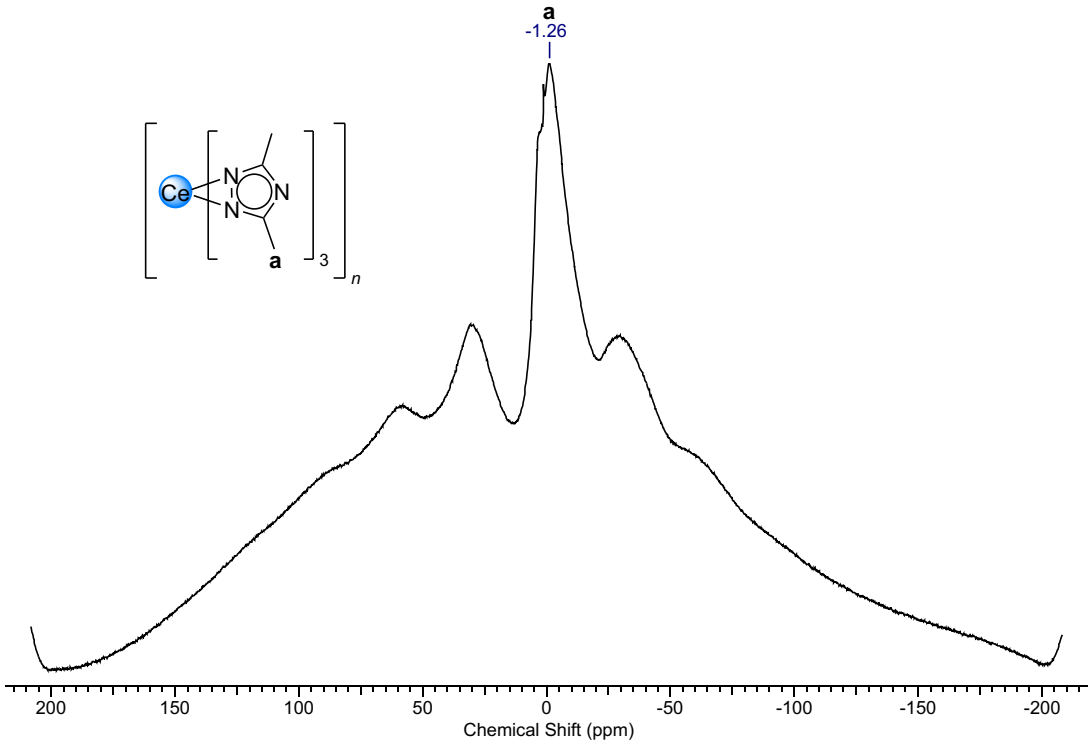

Figure S6. ^{1}H MAS NMR spectrum (300.1 MHz, 26 °C, MAS at 8 kHz) of $[Ce(tz^{Me,Me})_3]_n$ (**1**).

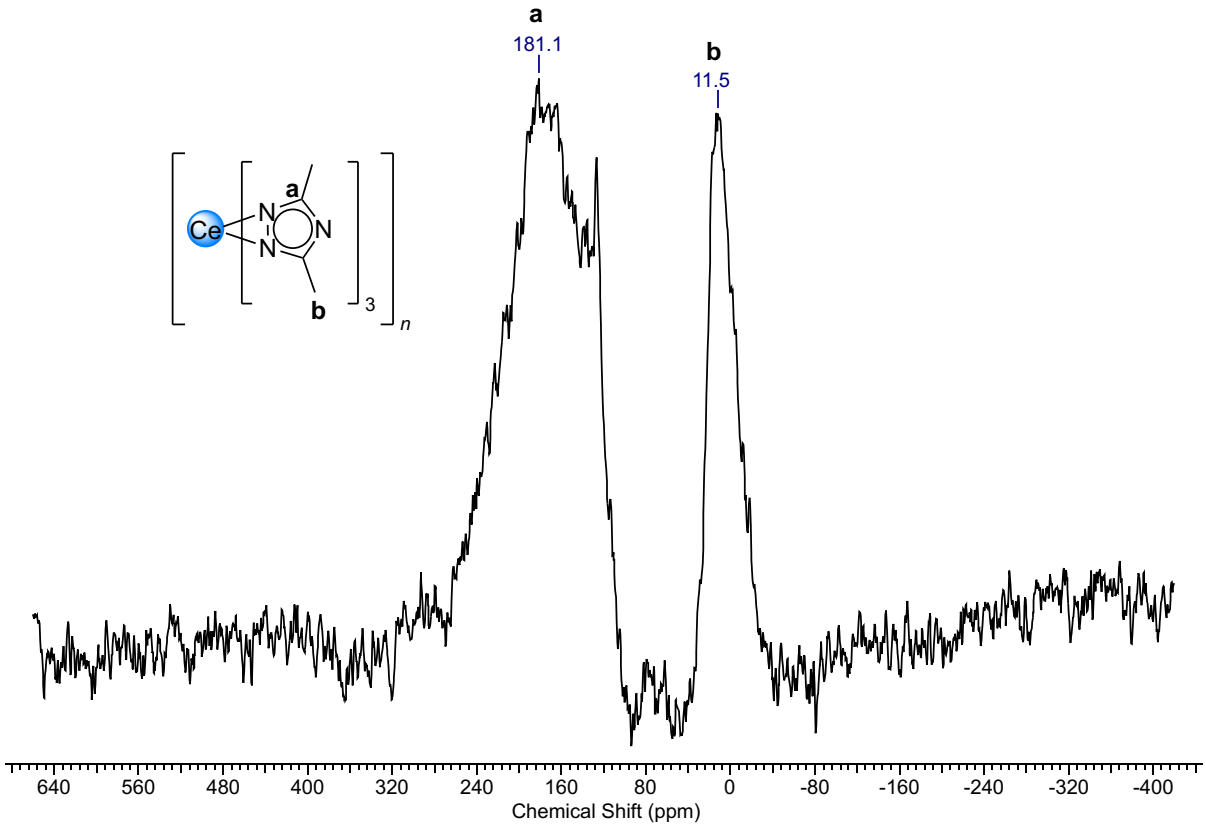

Figure S7. ^{13}C HPDEC MAS NMR spectrum (75.5 MHz, 24 °C, MAS at 8 kHz) of $[Ce(tz^{Me,Me})_3]_n$ (**1**).

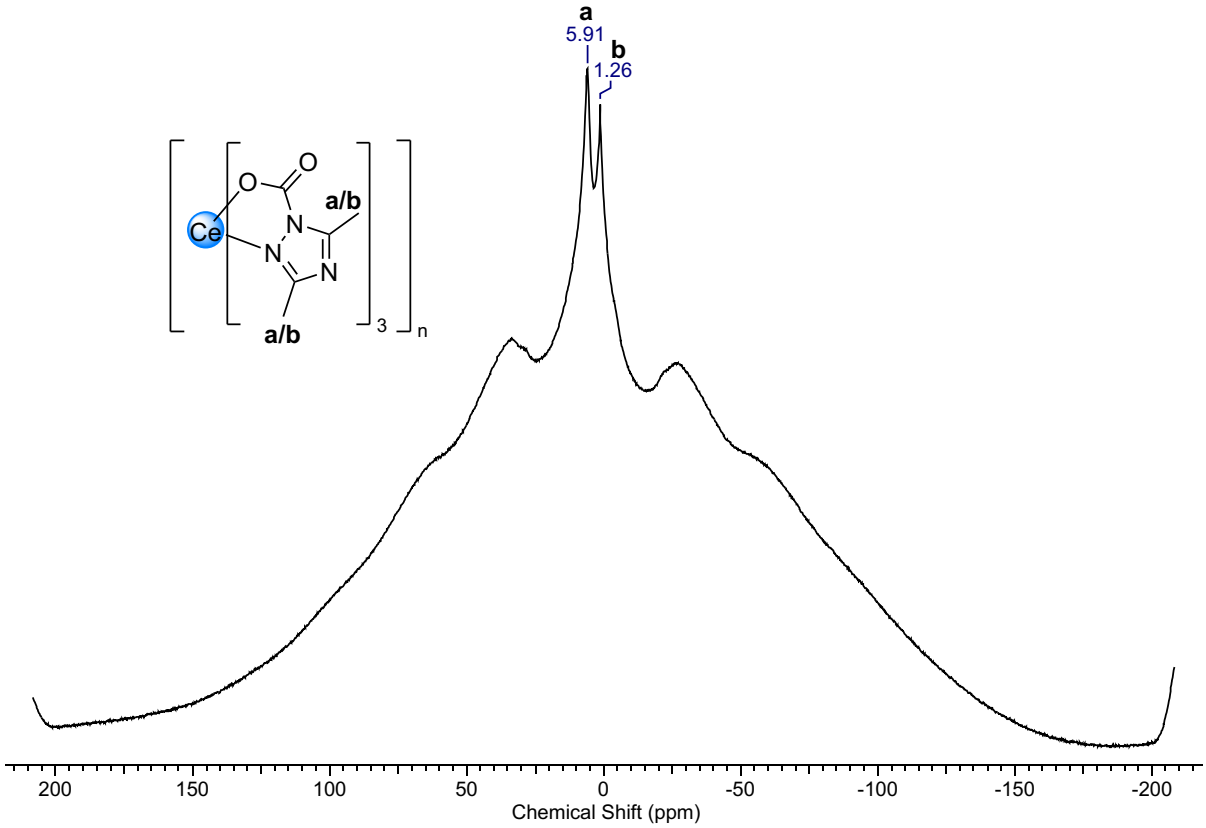

Figure S8. ^{1}H MAS NMR spectrum (300.1 MHz, 24 °C, MAS at 8 kHz) of $[Ce(tz^{Me,Me,13}CO_2)_3]_n$ (**1-$^{13}CO_2$**).

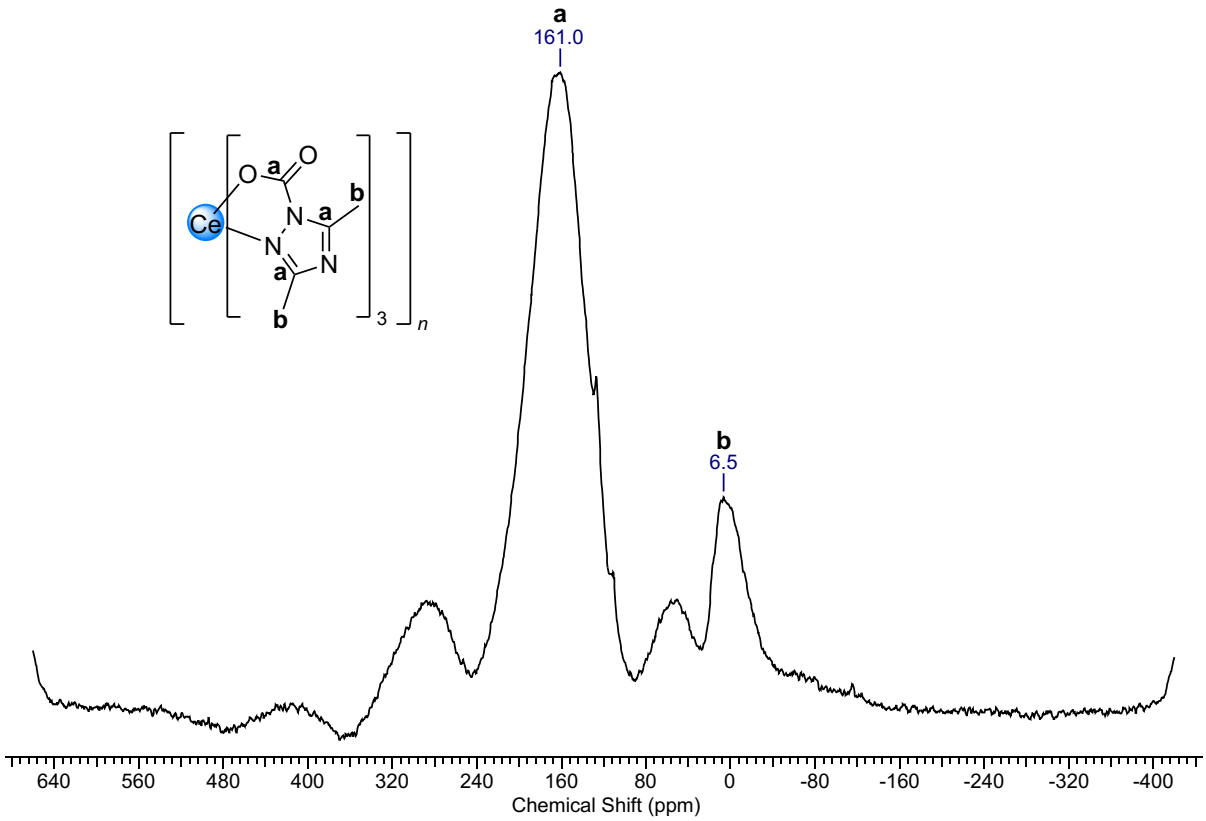

Figure S9. ^{13}C HPDEC MAS NMR spectrum (75.5 MHz, 25 °C, MAS at 8 kHz) of $[Ce(tz^{Me,Me,13}CO_2)_3]_n$ (**1-$^{13}CO_2$**).

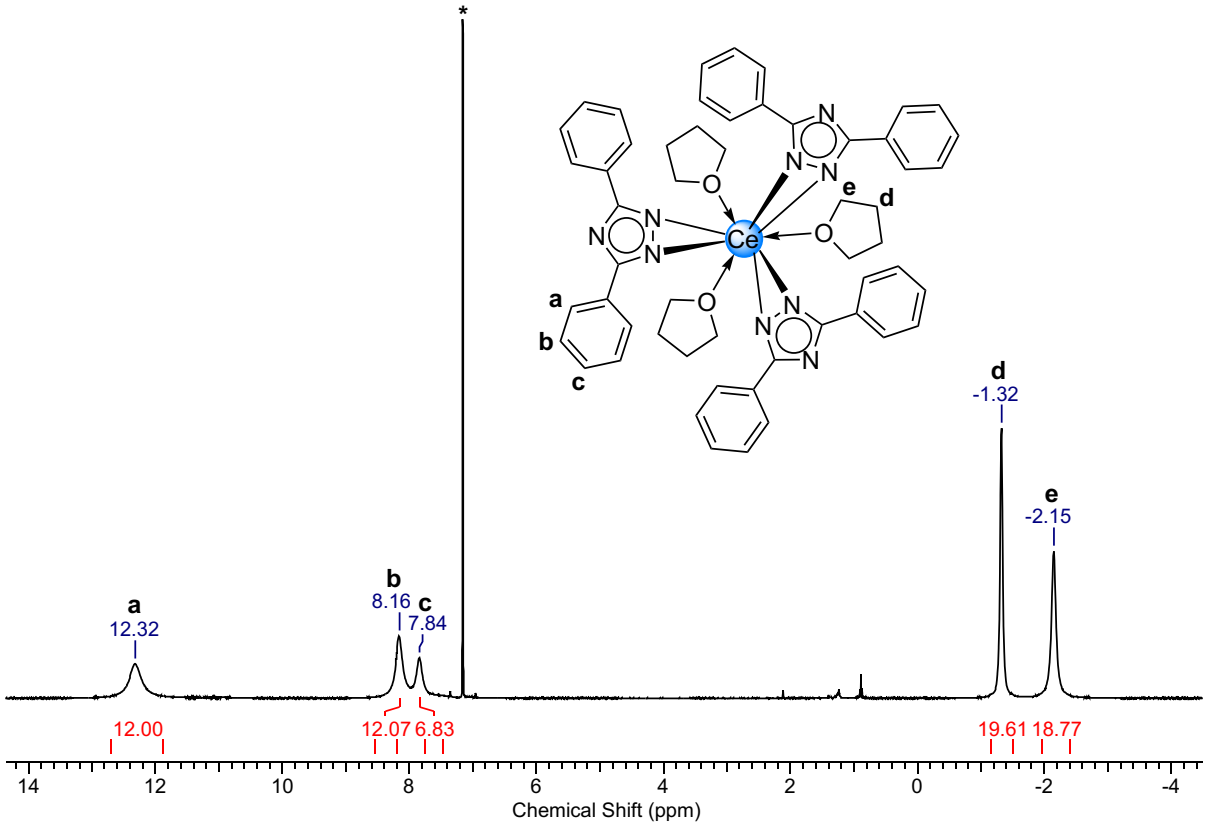

Figure S10. ^{1}H NMR spectrum (C_6D_6, 400.1 MHz, 26 °C) of Ce(tz^{Ph,Ph})$_3$(thf)$_3$ (**2**).

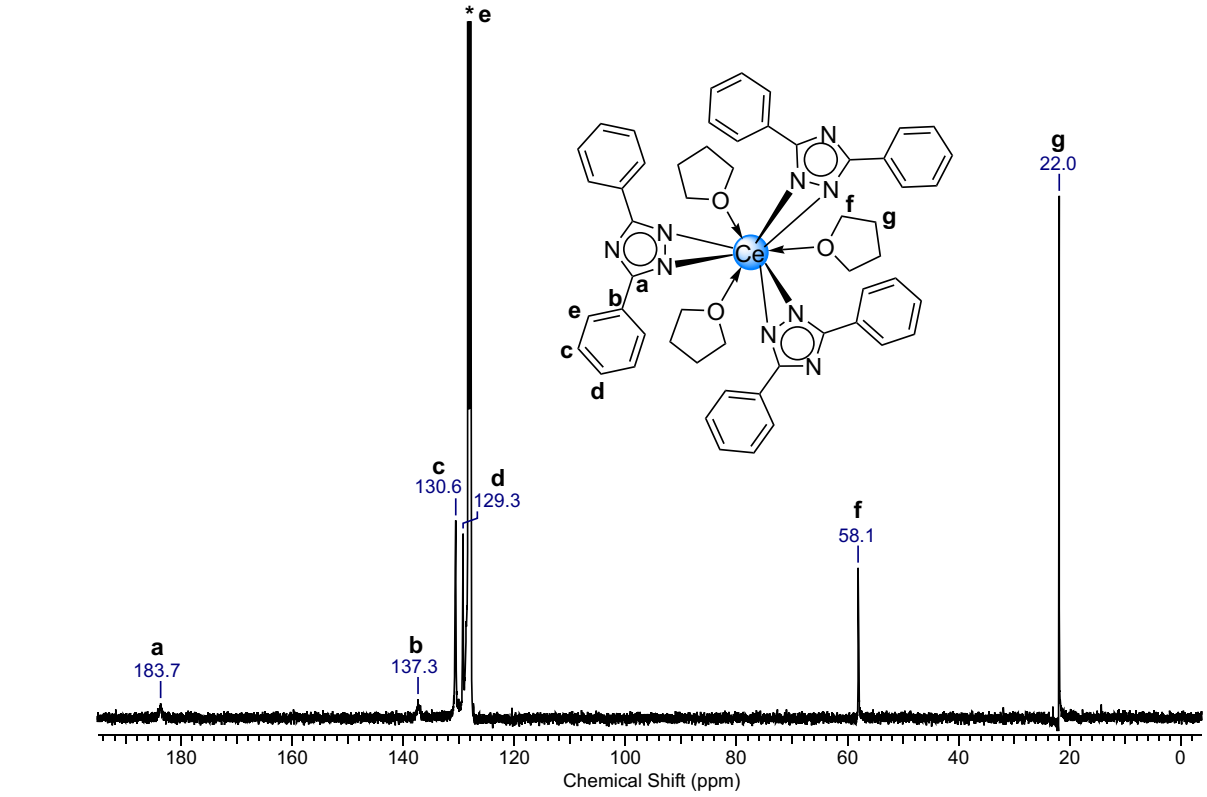

Figure S11. ^{13}C{^{1}H} NMR spectrum (C_6D_6, 100.6 MHz, 26 °C) of Ce(tz^{Ph,Ph})$_3$(thf)$_3$ (**2**).

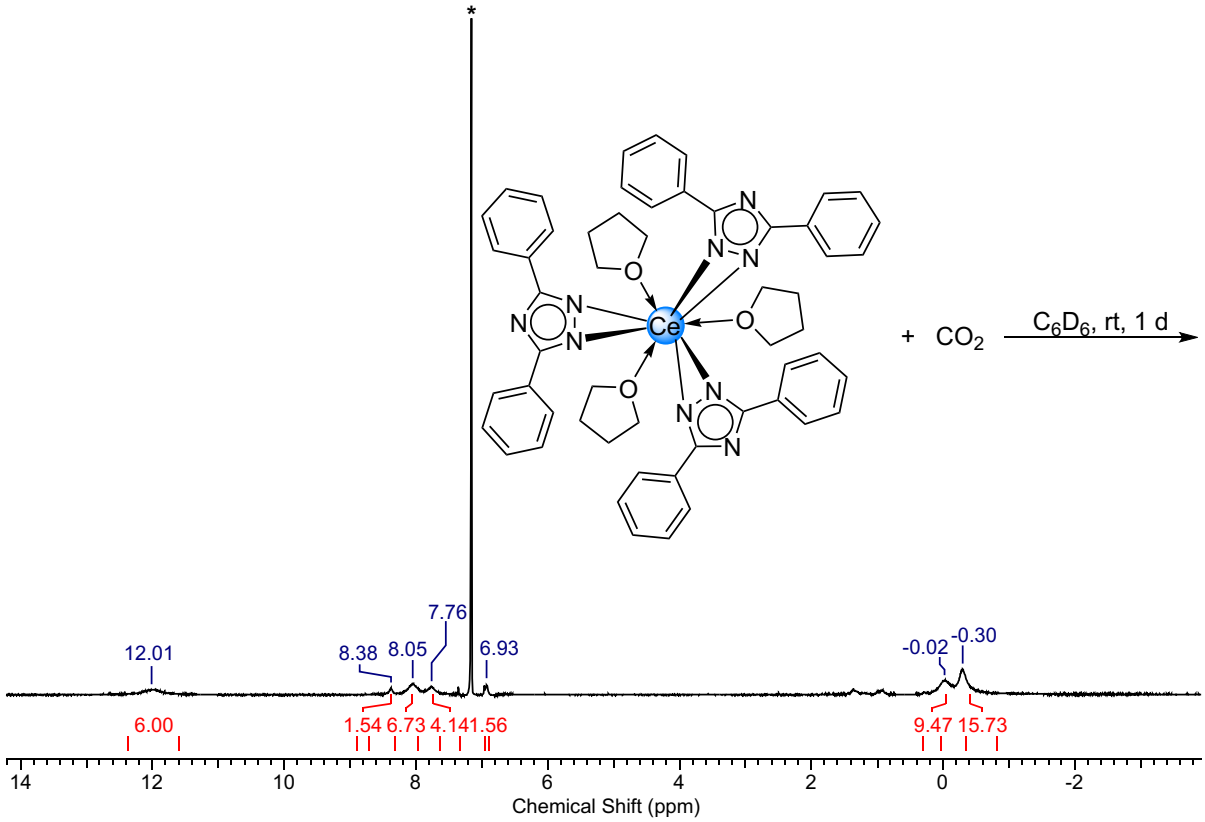

Figure S12. ^{1}H NMR spectrum (C_6D_6, 400.1 MHz, 26 °C) of the reaction of $Ce(tz^{Ph,Ph})_3(thf)_3$ (**2**) and 1 bar of CO_2 after 1 d.

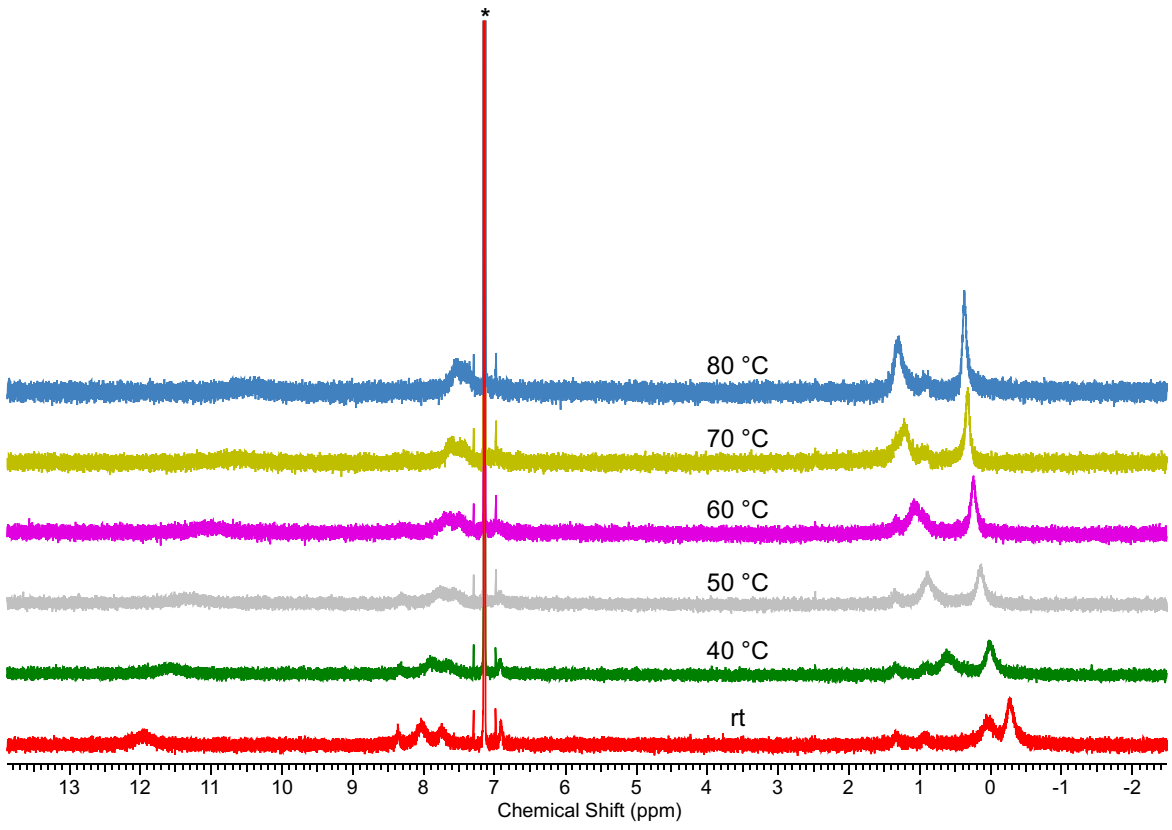

Figure S13. ^{1}H NMR spectra (C_6D_6, 500.1 MHz) of **2-CO$_2$** at different temperatures from ambient temperature up to 80 °C. Recooling to ambient temperature results in the same spectrum as before.

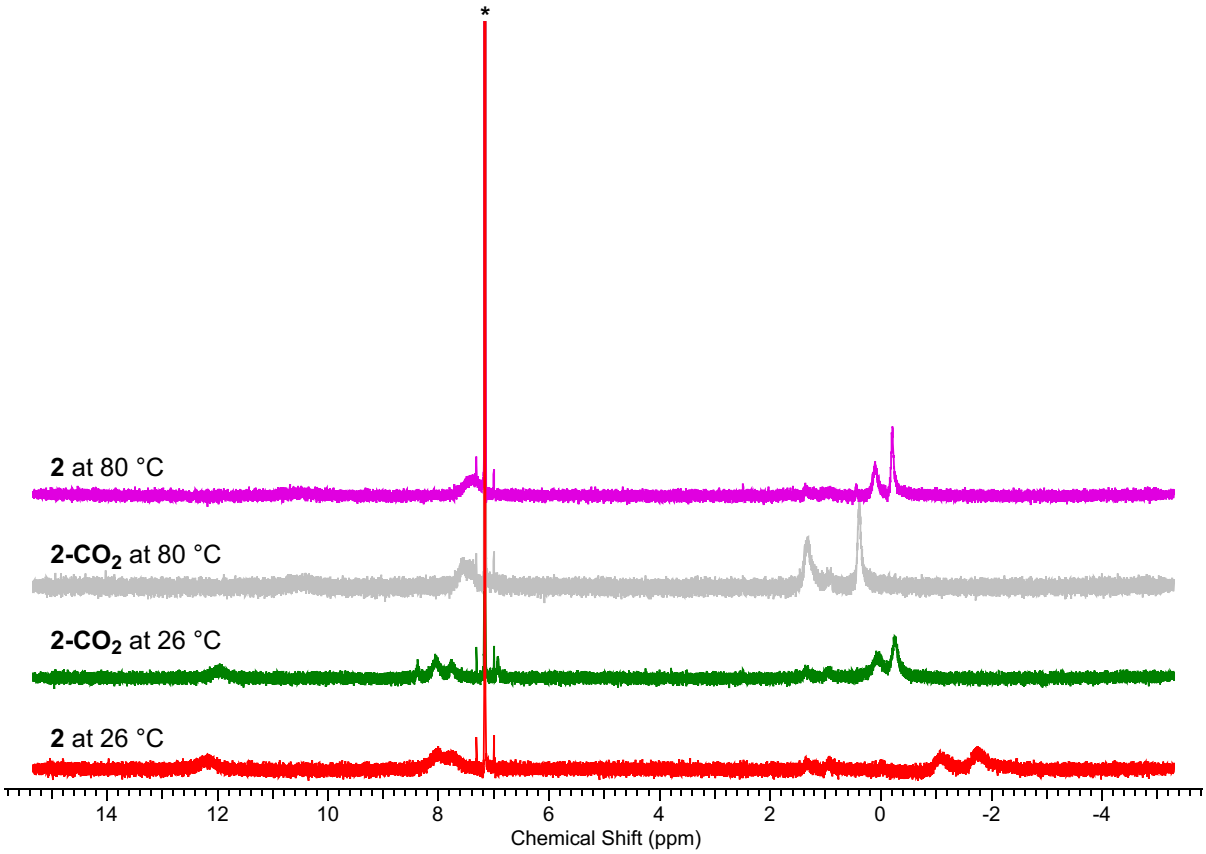

Figure S14. ^{1}H NMR spectra (C_6D_6, 500.1 MHz, 26 °C) of **2** and **2-CO$_2$** at ambient temperature and 80 °C.

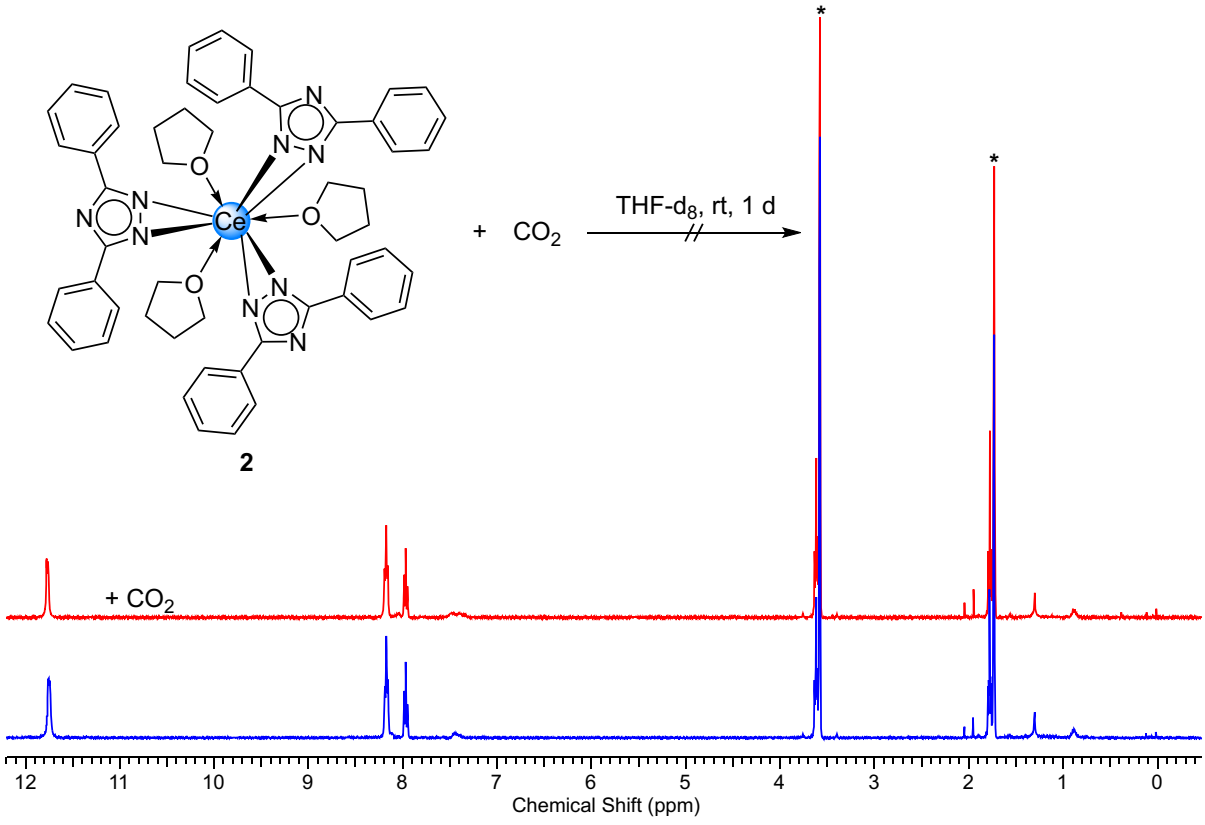

Figure S15. ^{1}H NMR spectra (THF-d_8, 400.1 MHz, 26 °C) of **2** and **2** upon CO_2 addition after one day.

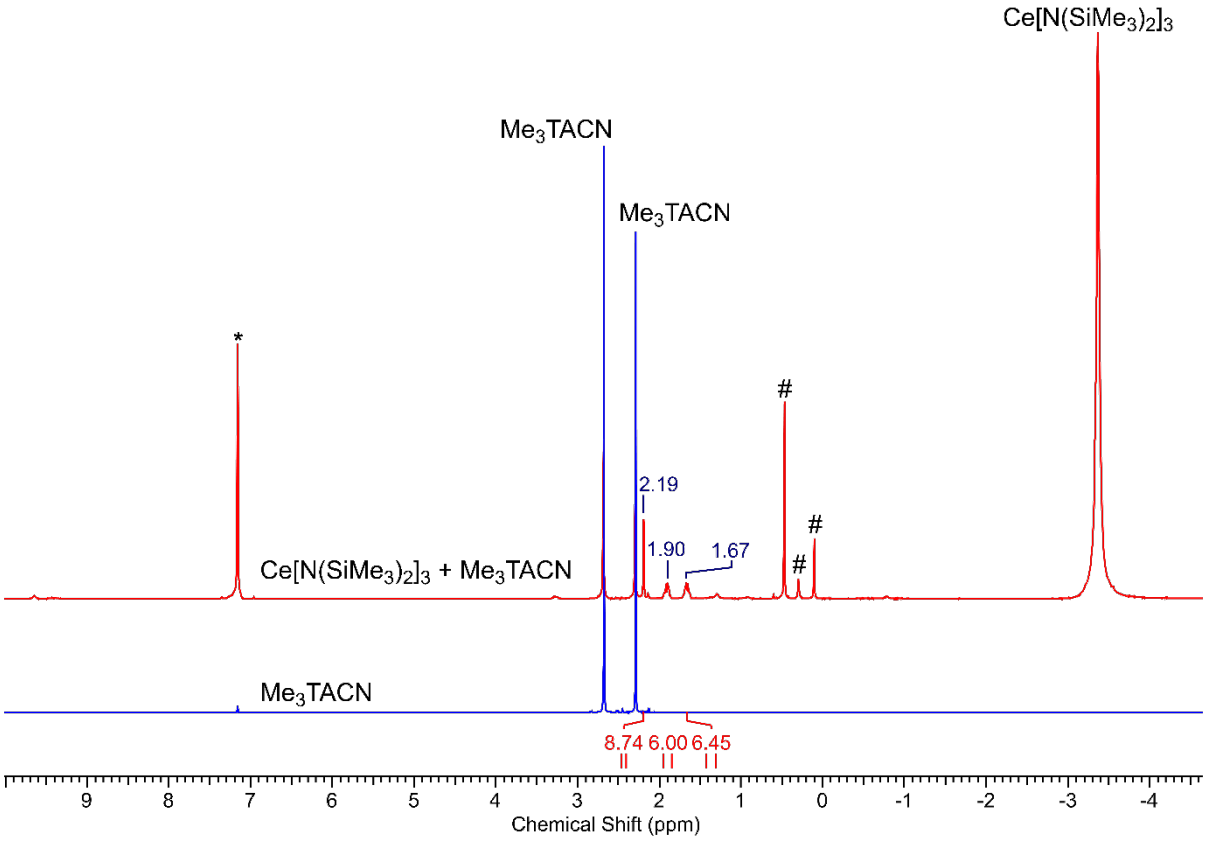

Figure S16. ^{1}H NMR spectra (C_6D_6, 400.1 MHz, 26 °C) of Me_3TACN (bottom) and the reaction of $Ce[N(SiMe_3)_2]_3$ and Me_3TACN (top).

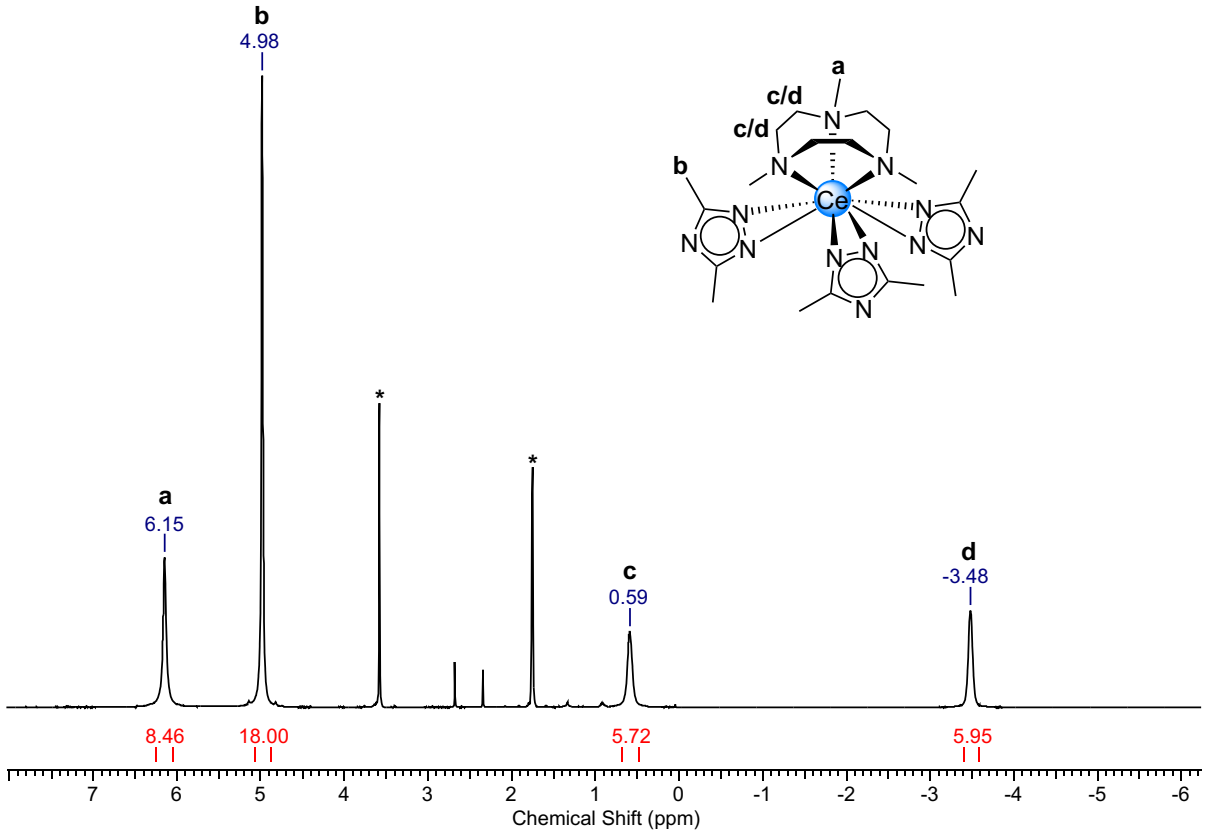

Figure S17. ^{1}H NMR spectrum (THF-d_8, 400.1 MHz, 26 °C) of $(Me_3TACN)Ce(tz^{Me,Me})_3(thf)$(**5**).

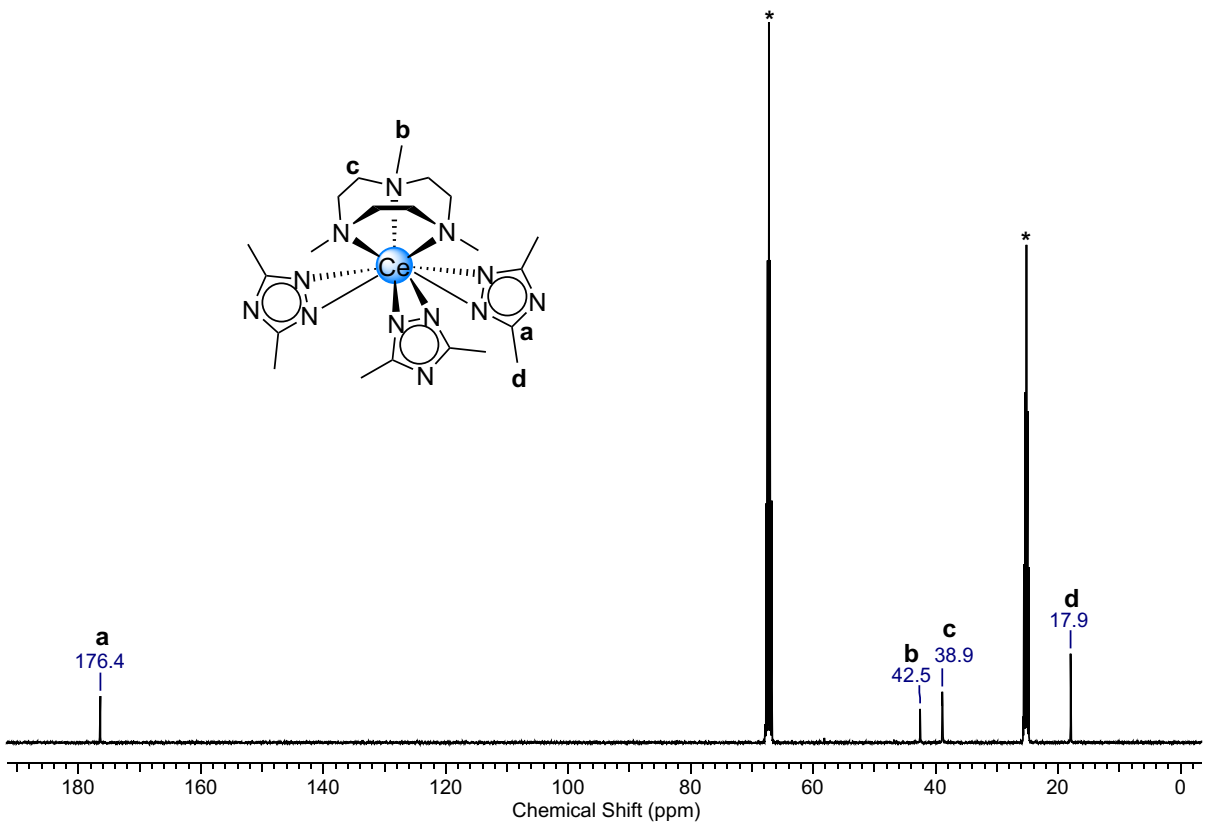

Figure S18. $^{13}C\{^{1}H\}$ NMR spectrum (THF-d_8, 100.6 MHz, 26 °C) of (Me_3TACN)Ce($tz^{Me,Me}$)$_3$ (**5**).

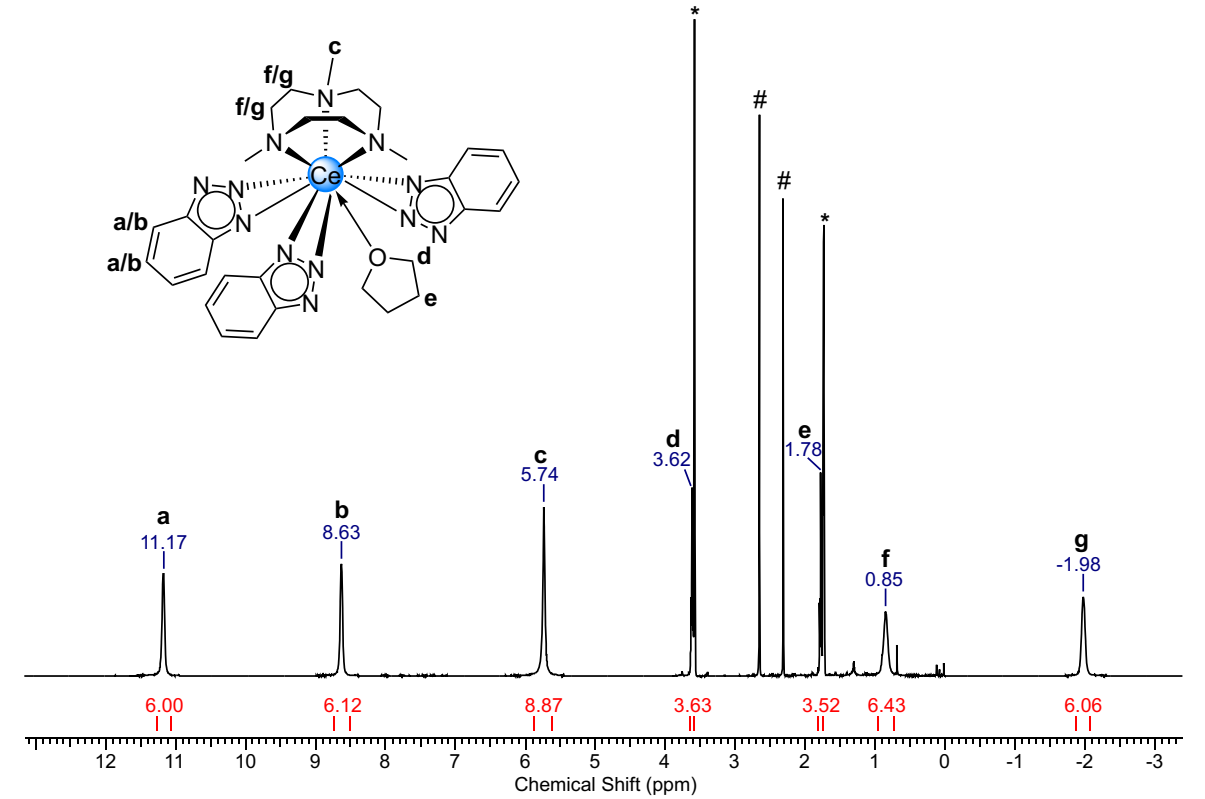

Figure S19. ^{1}H NMR spectrum (THF-d_8, 400.1 MHz, 26 °C) of (Me_3TACN)Ce(trz^{Bz})$_3$(thf) (**6**). # marks signals of free Me_3TACN.

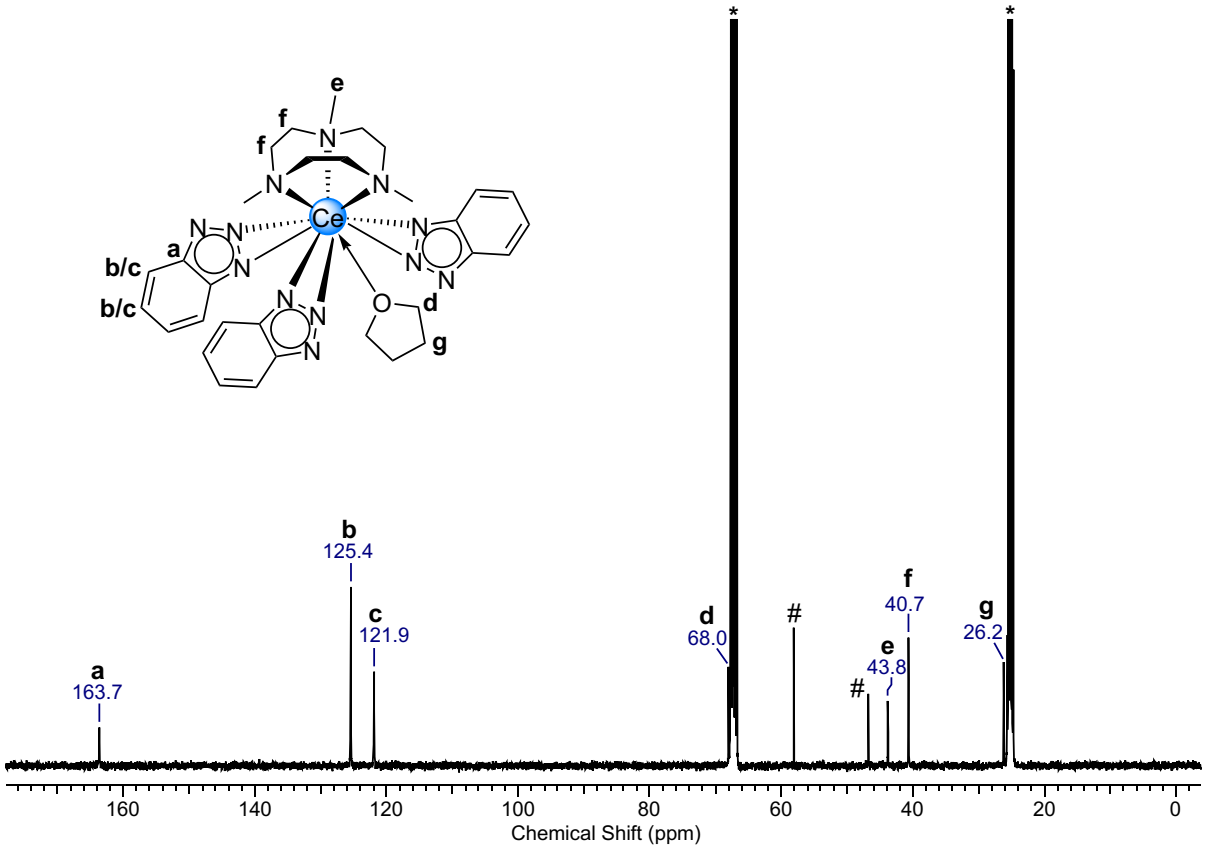

Figure S20. $^{13}C\{^{1}H\}$ NMR spectrum (THF-d_8, 100.6 MHz, 26 °C) of (Me_3TACN)Ce(trz^{Bz})$_3$(thf) (**6**). # marks signals of free Me_3TACN.

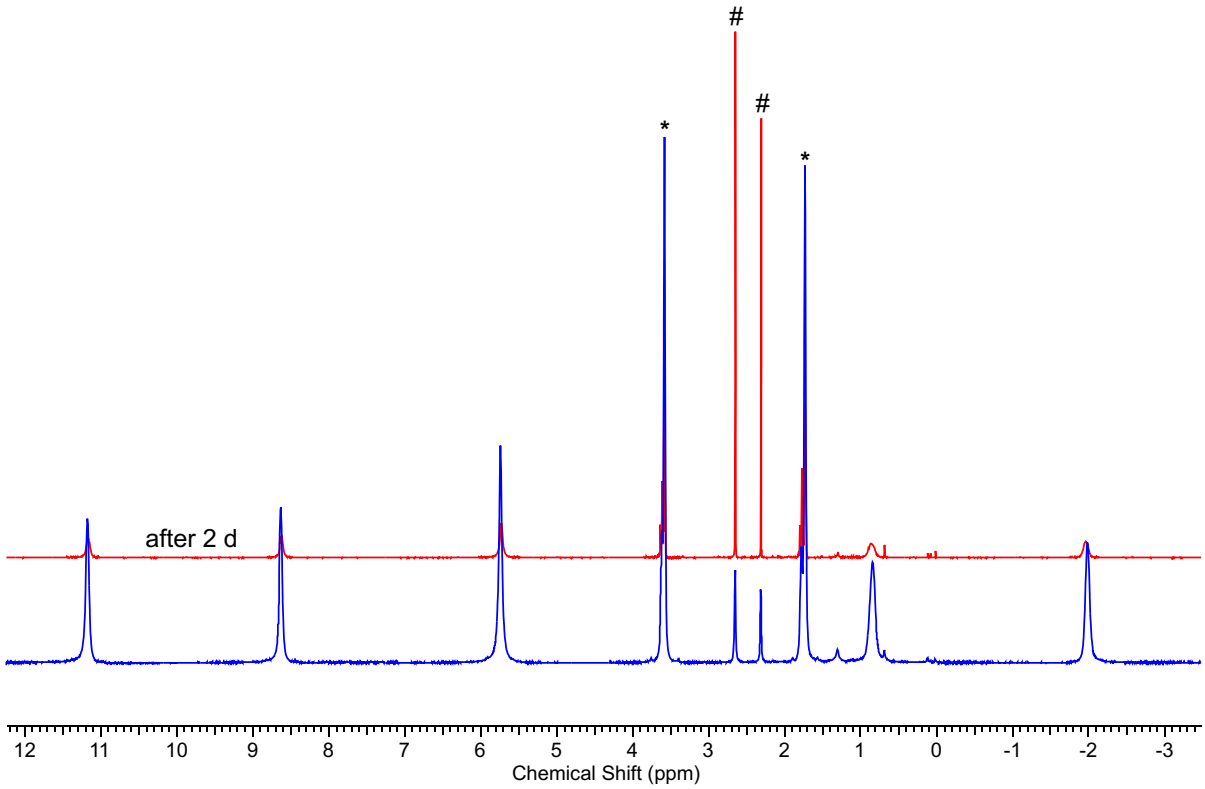

Figure S21. ^{1}H NMR spectra (THF-d_8, 400.1 MHz, 26 °C) of (Me_3TACN)Ce(trz^{Bz})$_3$(thf) (**6**) after dissolution (bottom) and after two days (top). # marks signals of free Me_3TACN.

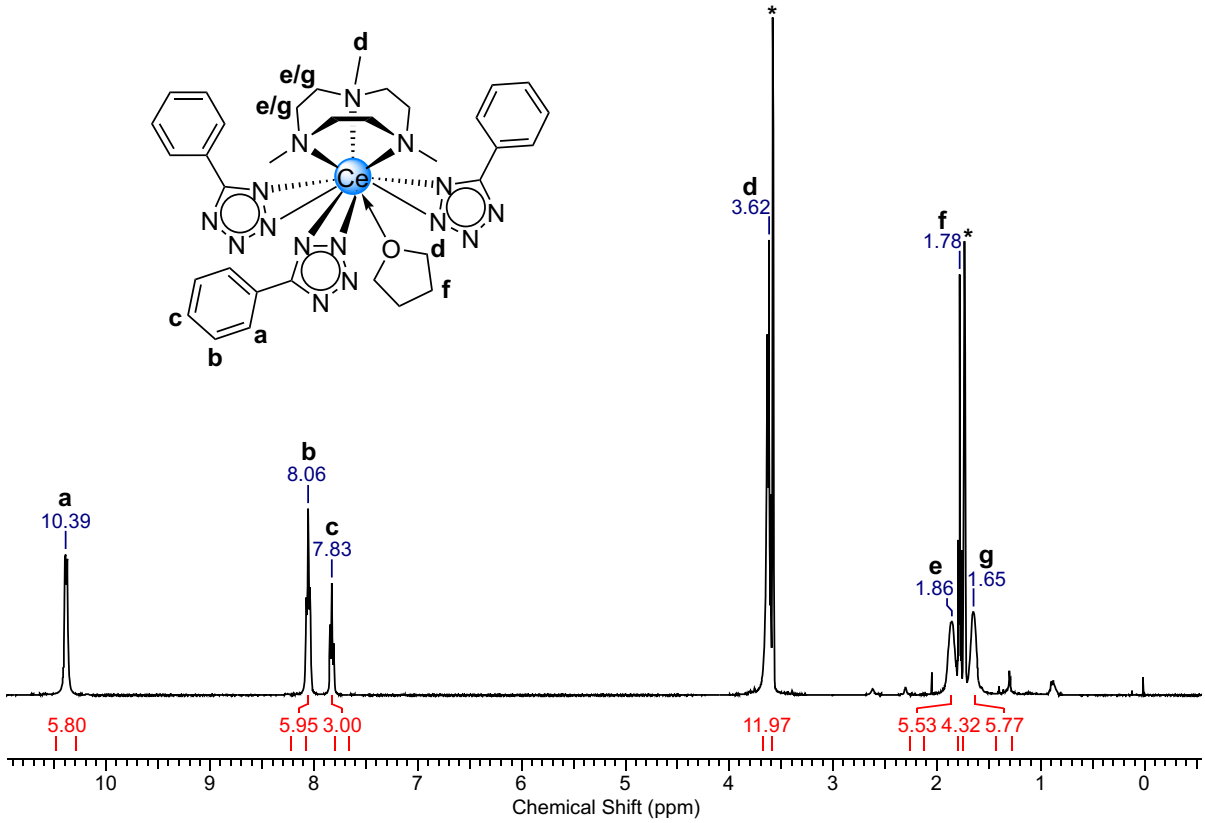

Figure S22. ^{1}H NMR spectrum (THF-d_8, 400.1 MHz, 26 °C) of (Me_3TACN)Ce(tet^{Ph})$_3$(thf) (**7**).

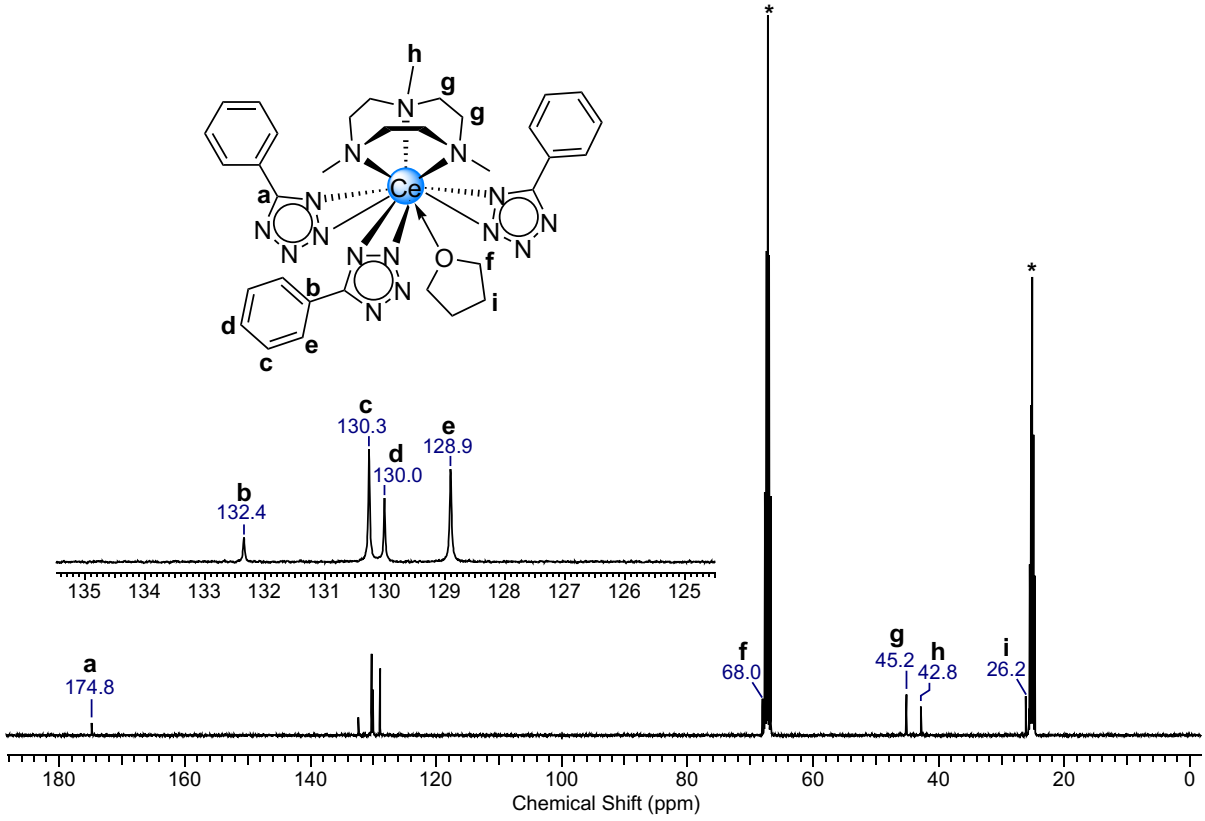

Figure S23. ^{13}C{^{1}H} NMR spectrum (THF-d_8, 100.6 MHz, 26 °C) of (Me_3TACN)Ce(tet^{Ph})$_3$(thf) (**7**).

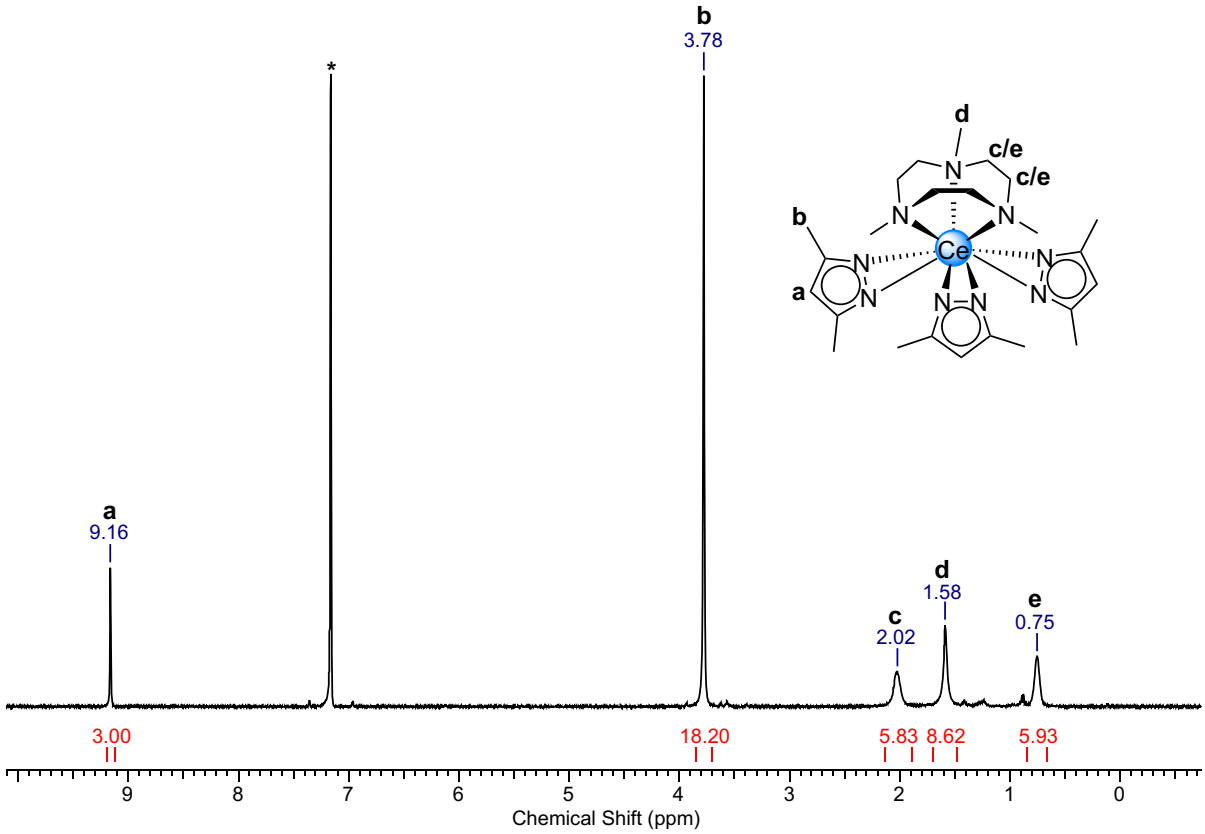

Figure S24. ^{1}H NMR spectrum (C_6D_6, 400.1 MHz, 26 °C) of $(Me_3TACN)Ce(pz^{Me,Me})_3$ (**8**).

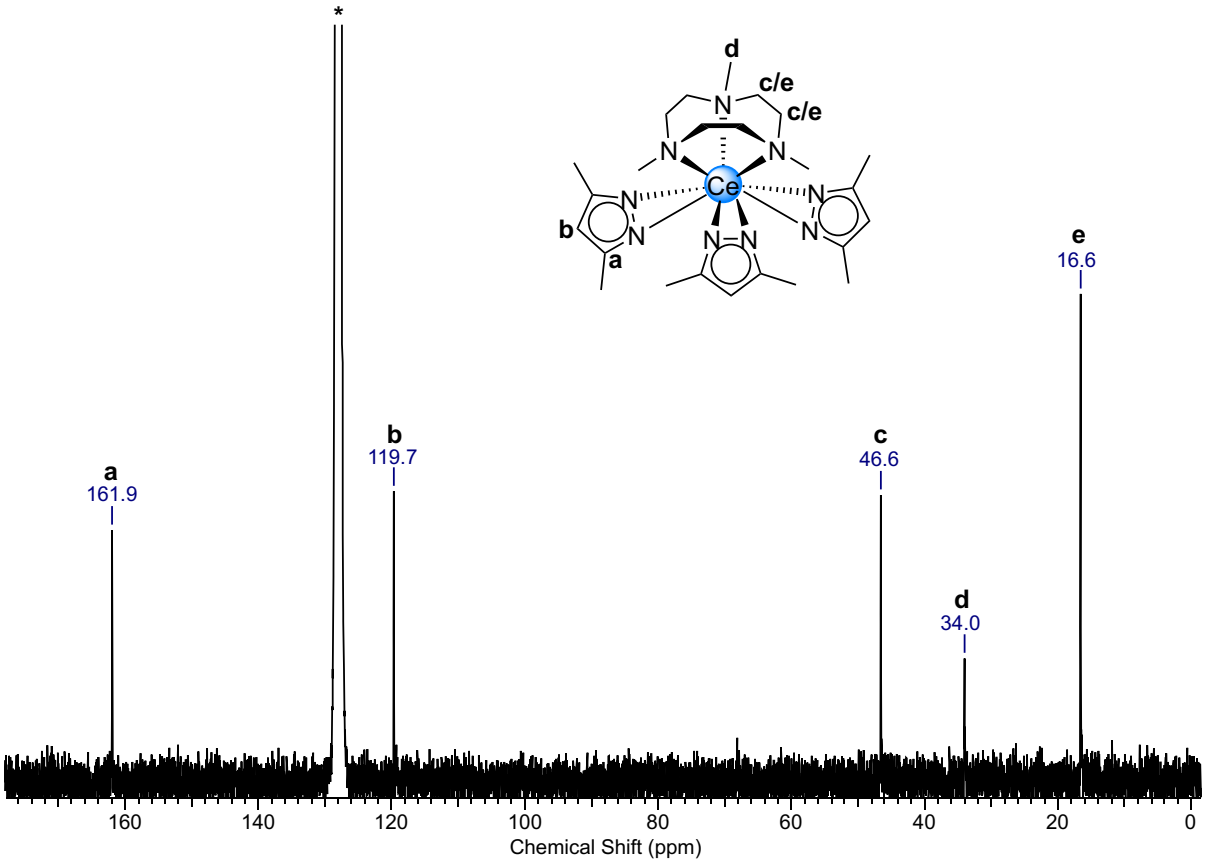

Figure S25. $^{13}C\{^{1}H\}$ NMR spectrum (C_6D_6, 100.6 MHz, 26 °C) of $(Me_3TACN)Ce(pz^{Me,Me})_3$ (**8**).

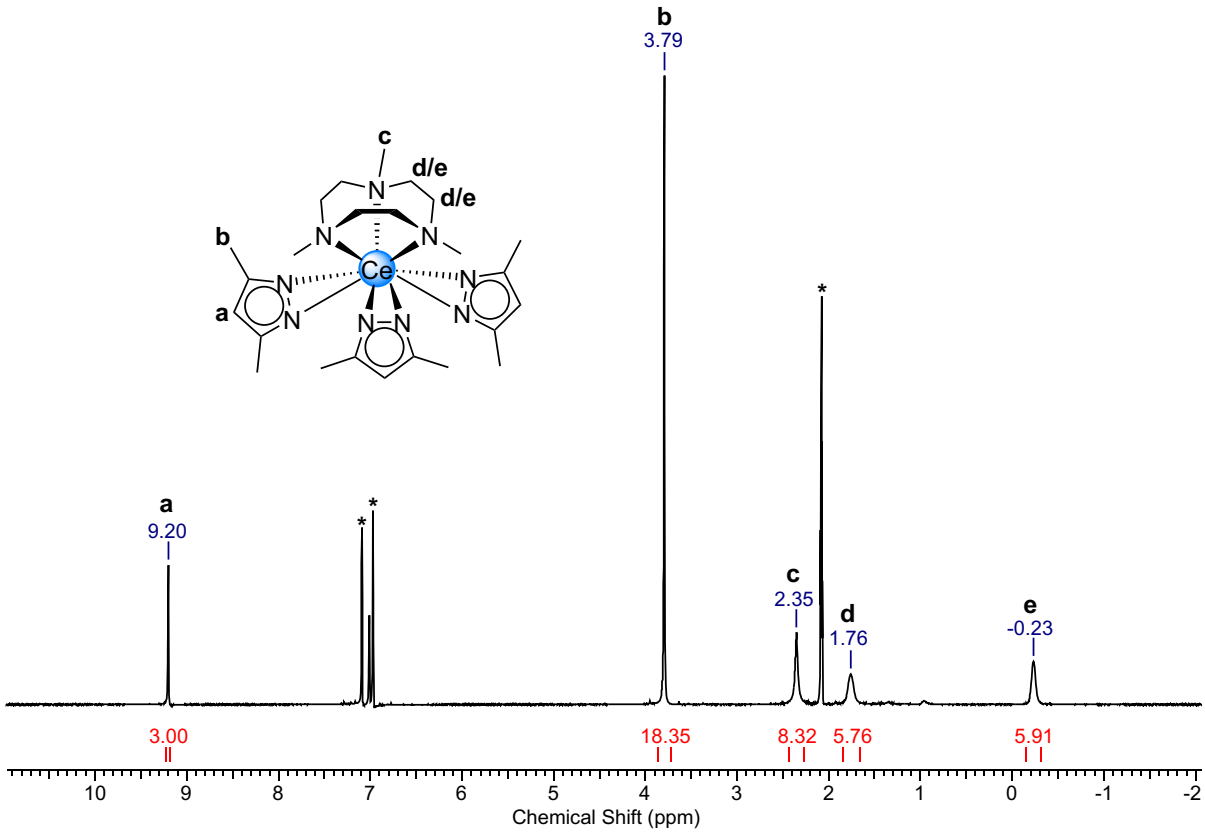

Figure S26. ^{1}H NMR spectrum (toluene-d_8, 400.1 MHz, 26 °C) of (Me_3TACN)Ce($pz^{Me,Me}$)$_3$ (**8**).

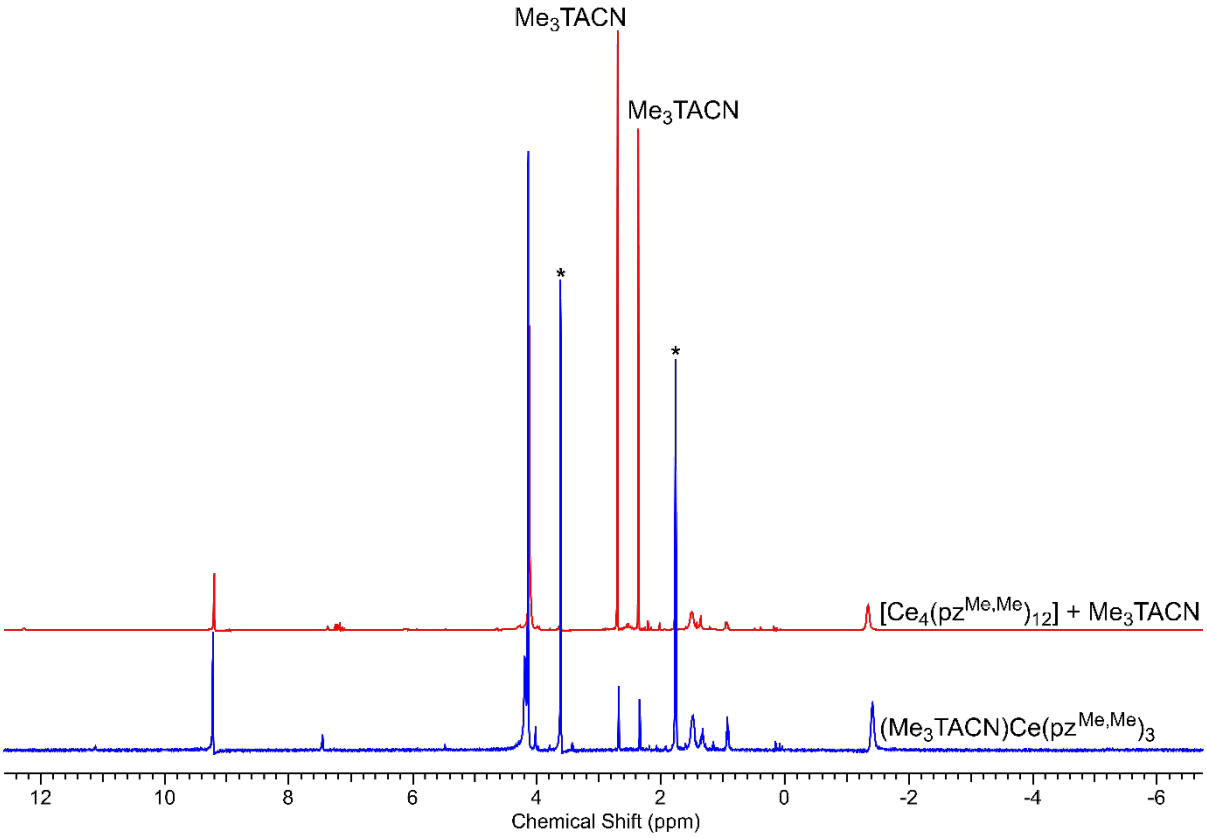

Figure S27. ^{1}H NMR spectrum (THF-d_8, 400.1 MHz) of (Me_3TACN)Ce($pz^{Me,Me}$)$_3$ (**8**, bottom, 26 °C) and of the reaction of [Ce_4($pz^{Me,Me}$)$_{12}$] and Me_3TACN (top, 27 °C).

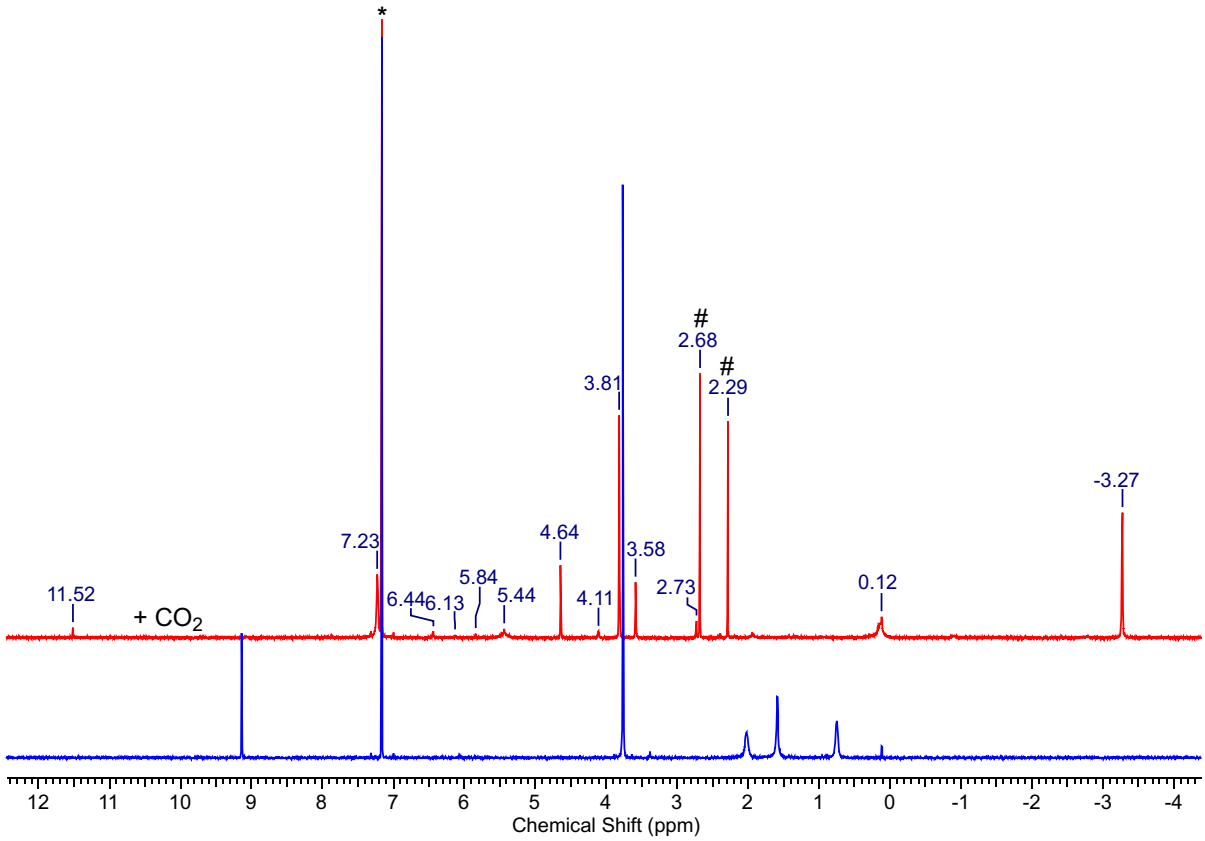

Figure S28. ^{1}H NMR spectra (C_6D_6, 500.1 MHz, 26 °C) of (Me_3TACN)Ce($pz^{Me,Me}$)$_3$ before (**8**, bottom) and after the reaction with CO_2 (top). # marks signals of Me_3TACN.

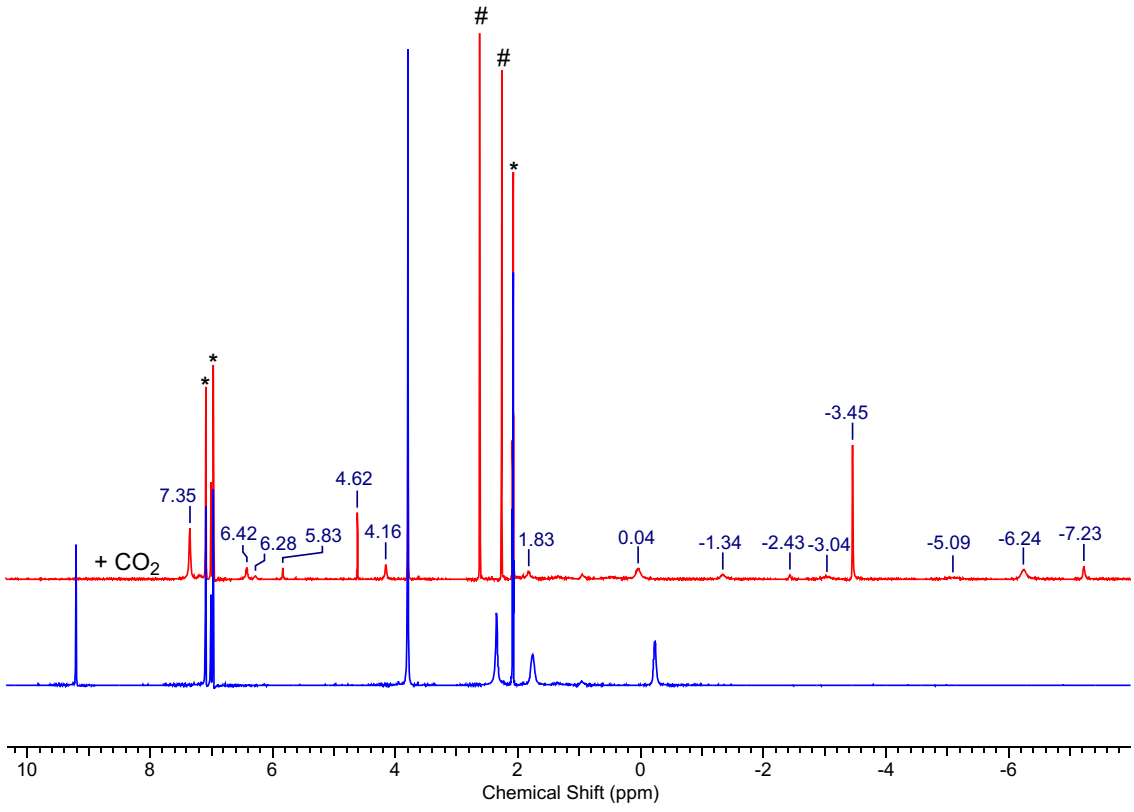

Figure S29. ^{1}H NMR spectra (toluene-d_8, 400.1 MHz, 26 °C) of Me_3TACN($pz^{Me,Me}$)$_3$ before (**8**, bottom) and after the reaction with CO_2 (top). # marks signals of Me_3TACN.

IR Spectra

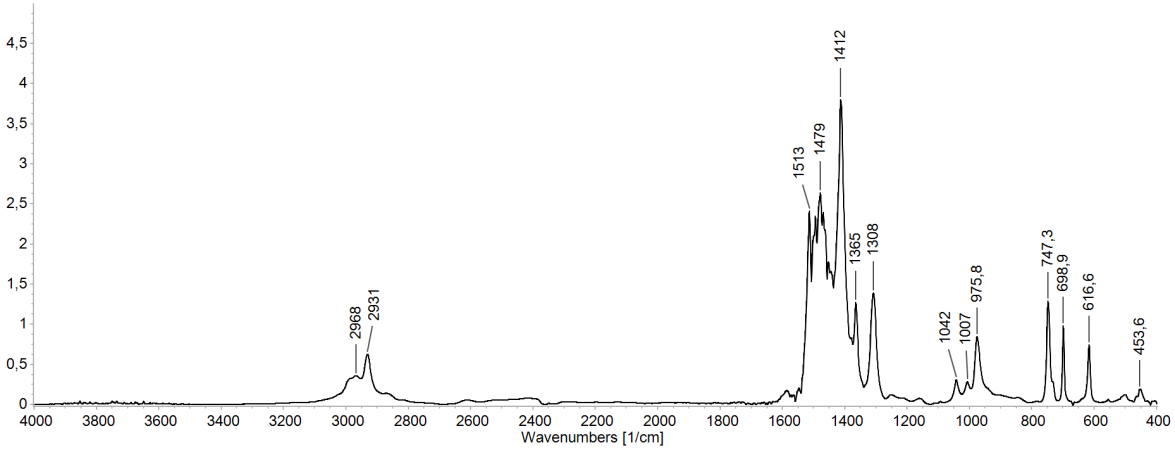

Figure S30. DRIFT spectrum of $[Ce(tz^{Me,Me})_3]_n$ (**1**).

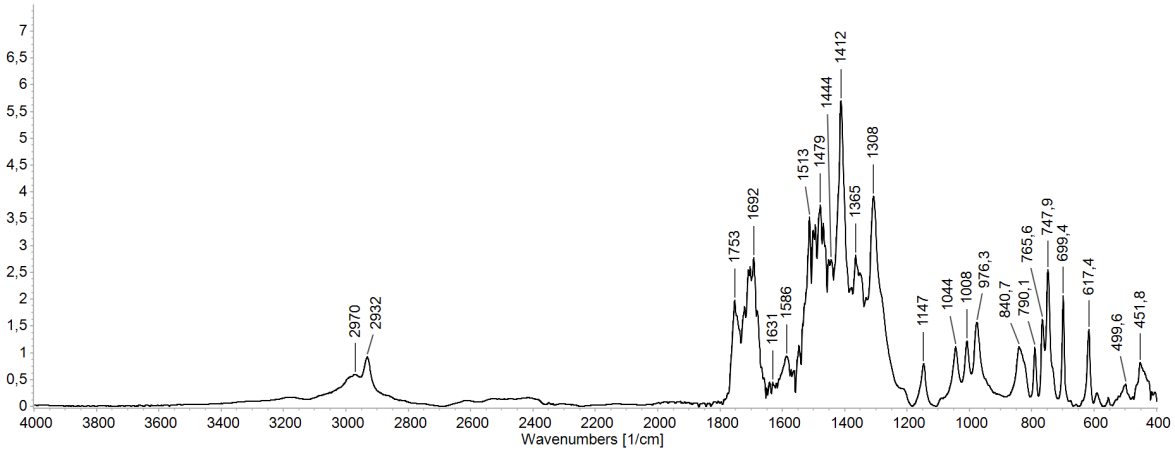

Figure S31. DRIFT spectrum of $[Ce(tz^{Me,Me}\cdot CO_2)_3]_n$ (**1-CO₂**).

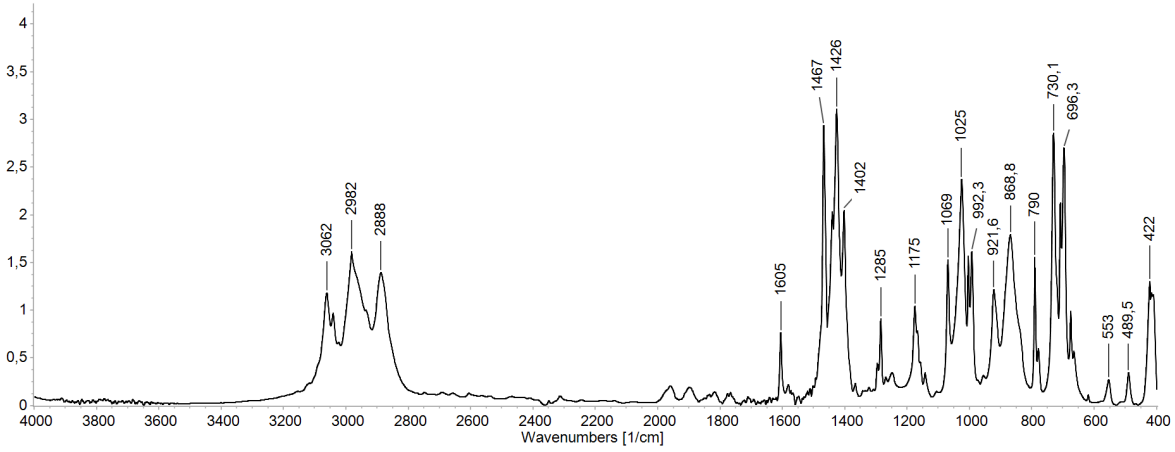

Figure S32. DRIFT spectrum of $Ce(tz^{Ph,Ph})_3(thf)_3$ (**2**).

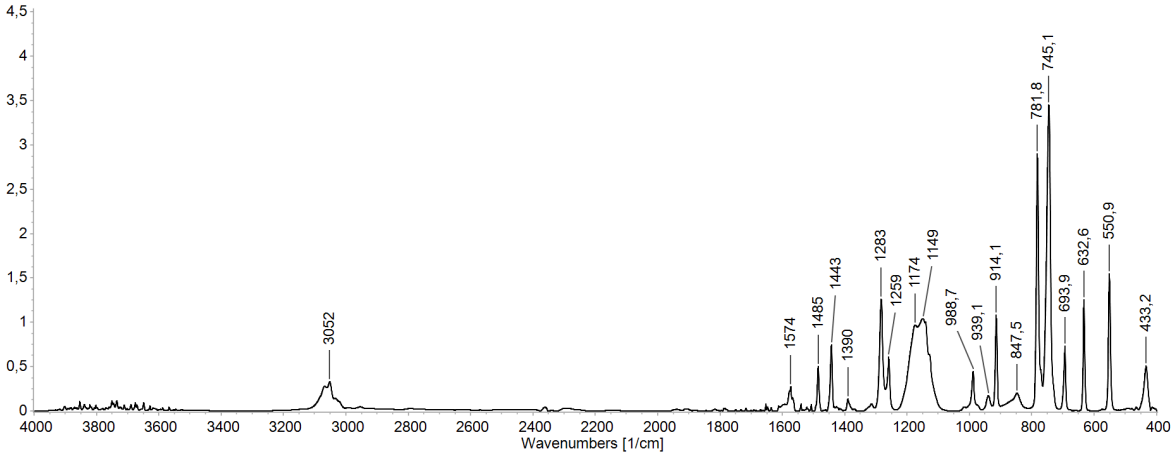

Figure S33. DRIFT spectrum of $[Ce(trz^{Bz})_3]_n$ (**3**).

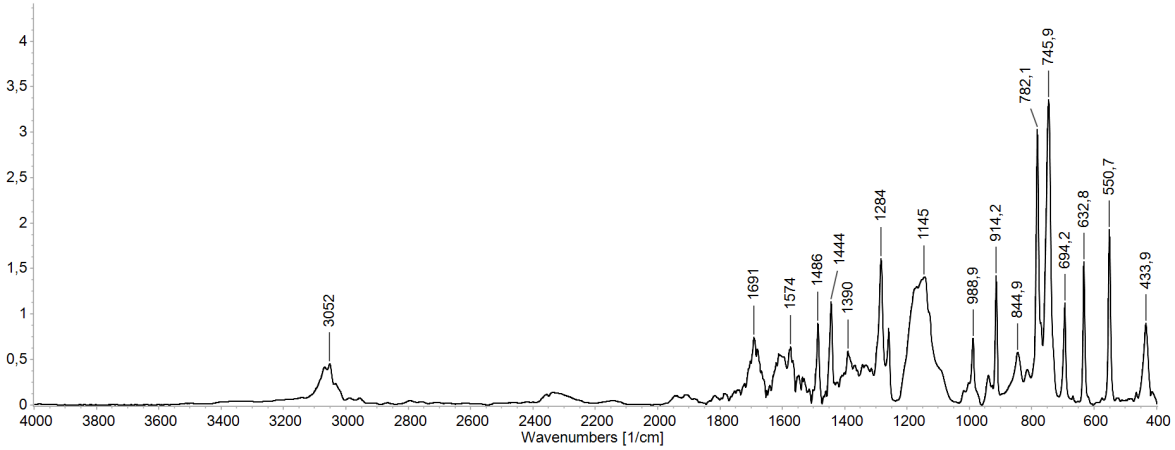

Figure S34. DRIFT spectrum of $[Ce(trz^{Bz}{\cdot}CO_2)(trz^{Bz})_2]_n$ (**3-CO₂**).

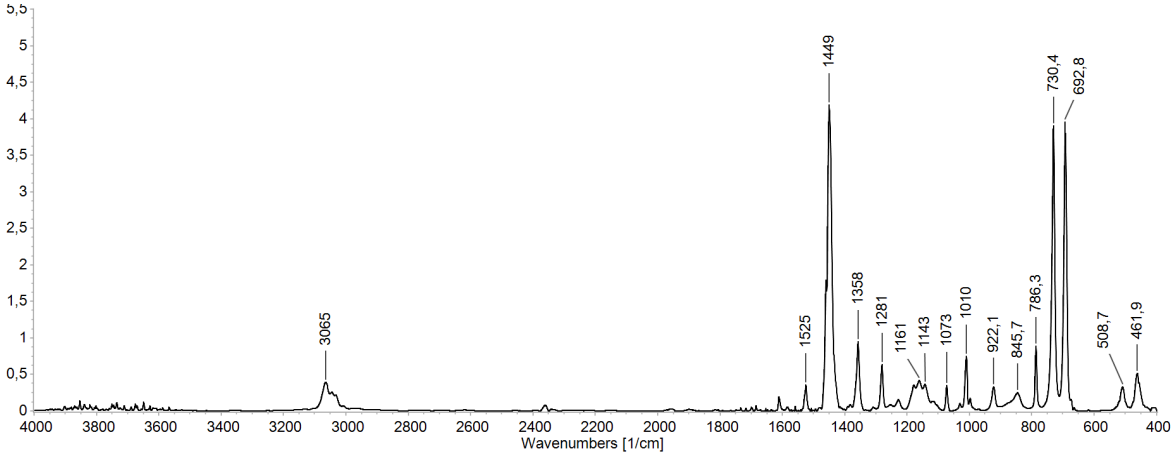

Figure S35. DRIFT spectrum of $[Ce(tet^{Ph})_3]_n$ (**4**).

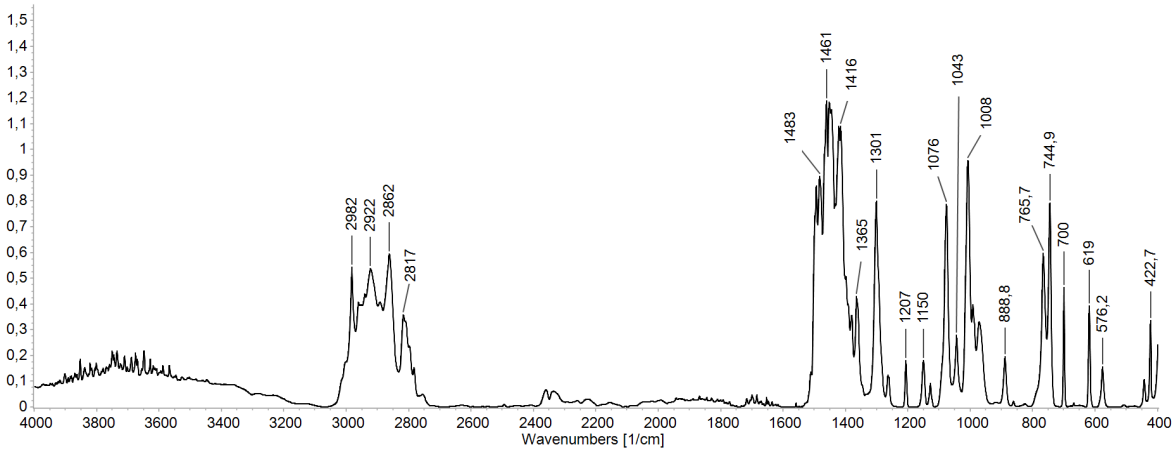

Figure S36. DRIFT spectrum of $(Me_3TACN)Ce(tz^{Me,Me})_3$ (**5**).

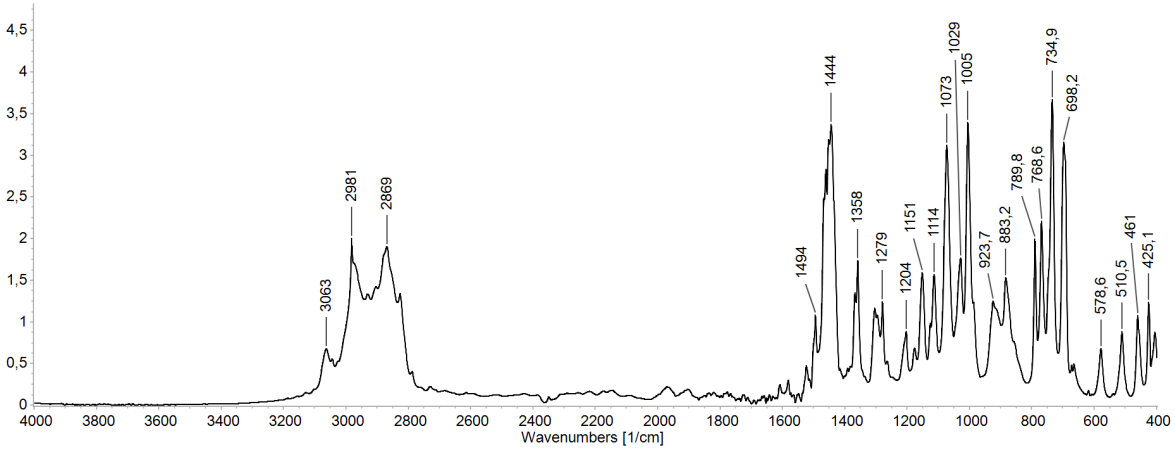

Figure S37. DRIFT spectrum of $(Me_3TACN)Ce(tet^{Ph})_3(thf)$ (**7**).

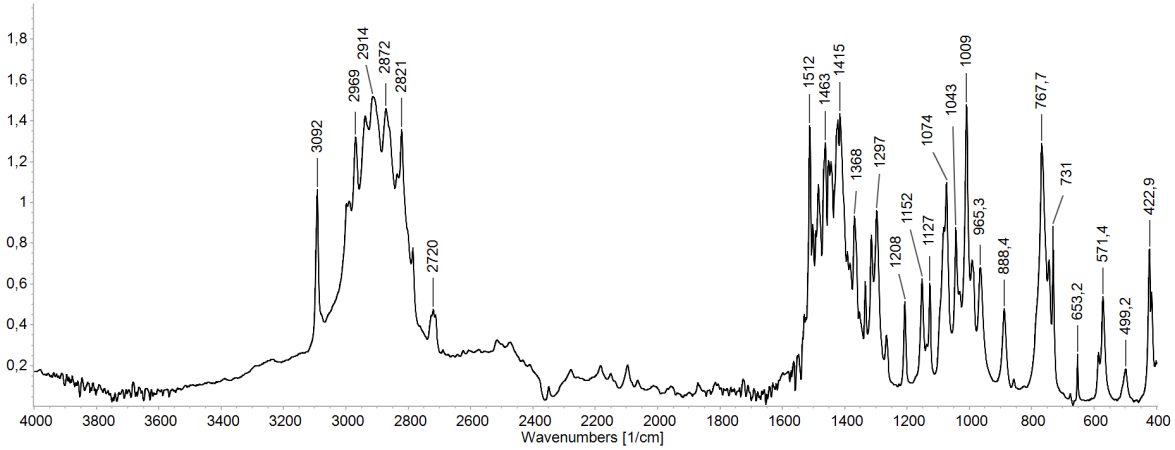

Figure S38. DRIFT spectrum of $(Me_3TACN)Ce(pz^{Me,Me})_3$ (**8**).

Thermogravimetric Analysis

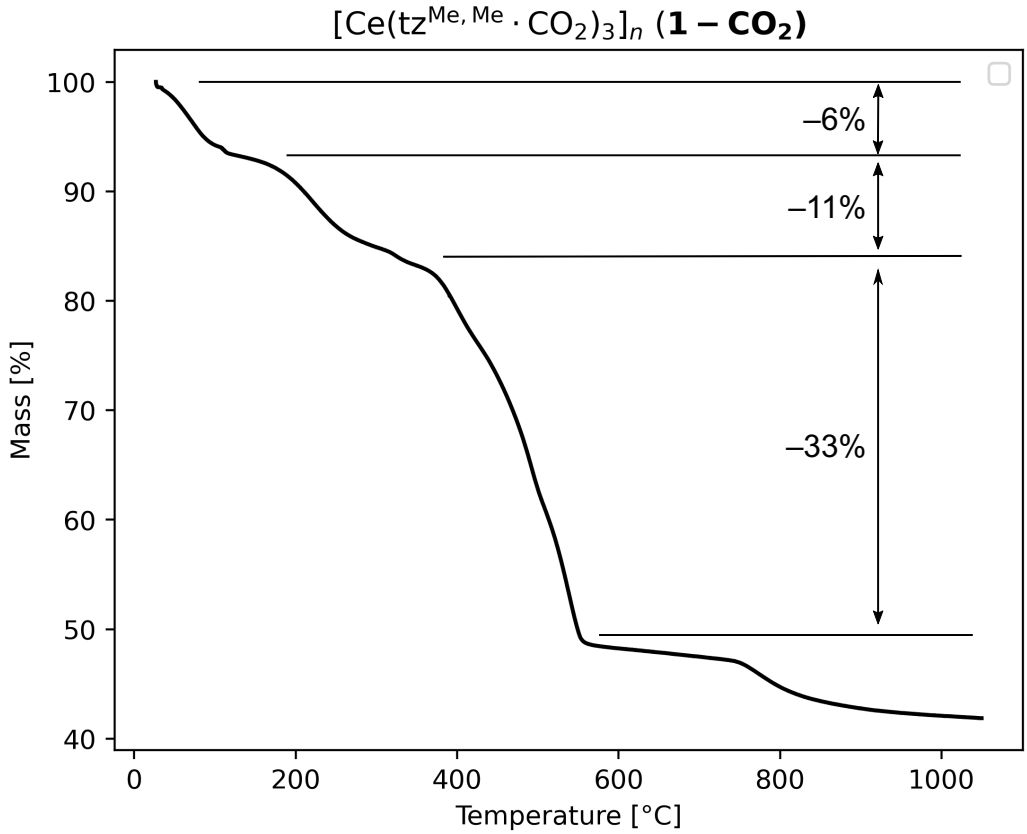

Figure S39. Thermogravimetric analysis of $[Ce(tz^{Me,Me}\cdot CO_2)_3]_n$ (**1-CO₂**). Sample was heated from 27 °C to 1050 °C with a heating ratio of 2 $Kmin^{-1}$ under constant Ar flow.

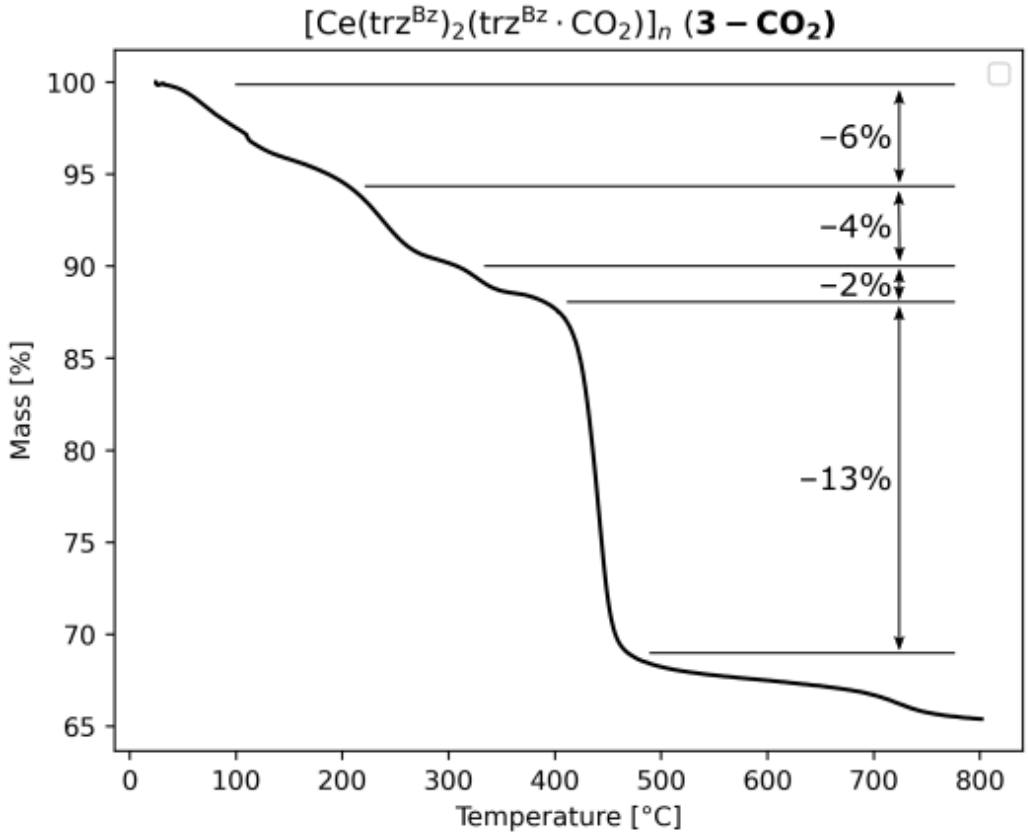

Figure S40. Thermogravimetric analysis of $[Ce(trz^{Bz})_2(trz^{Bz}\cdot CO_2)]_n$ (**3-CO₂**). Sample was heated from 25 °C to 800 °C with a heating ratio of 2 $Kmin^{-1}$ under constant Ar flow.

Absorption Spectra

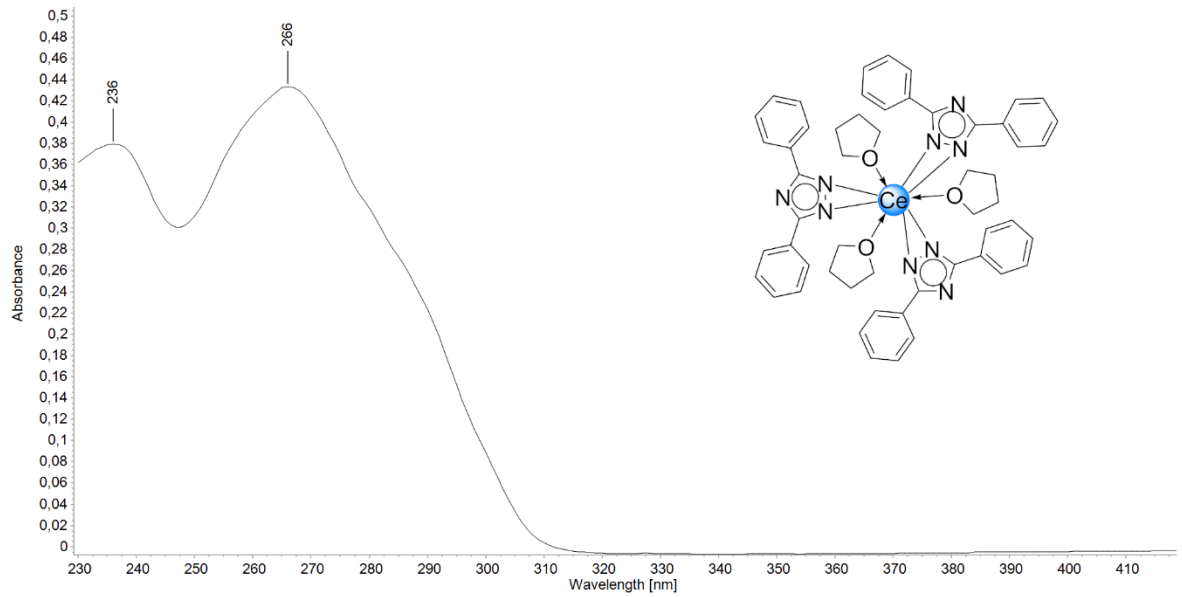

Figure S41. Absorption spectrum of a 10 µM solution of $Ce(tz^{Ph,Ph})_3(thf)_3$ (**2**) in THF.

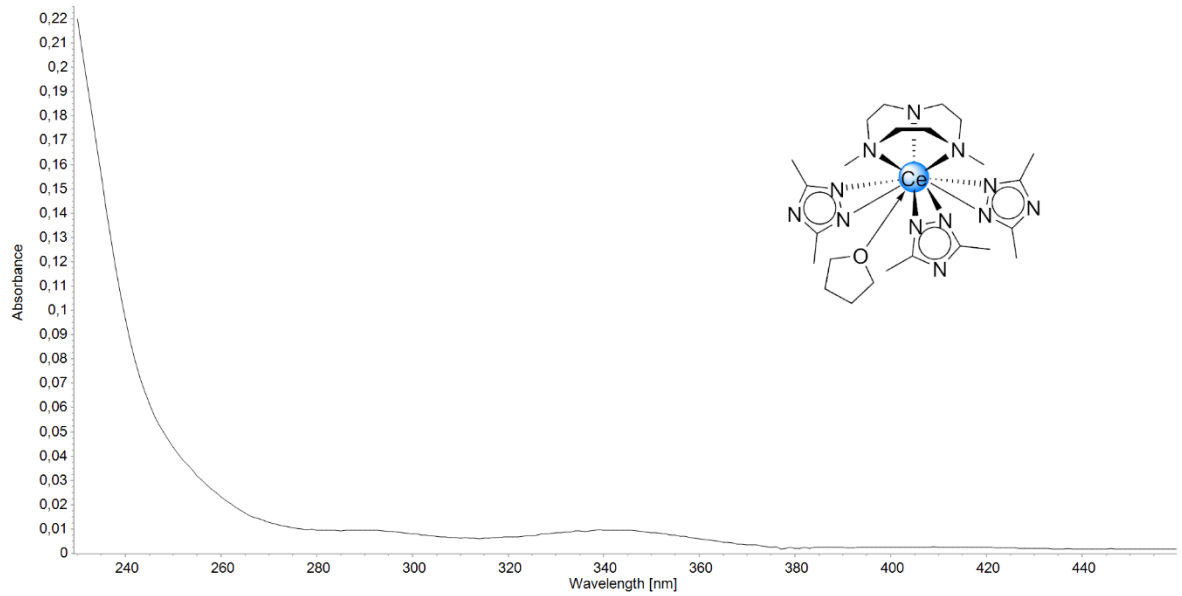

Figure S42. Absorption spectrum of a 20 µM solution of $(Me_3TACN)Ce(tz^{Me,Me})_3(thf)$ (**5**) in THF.

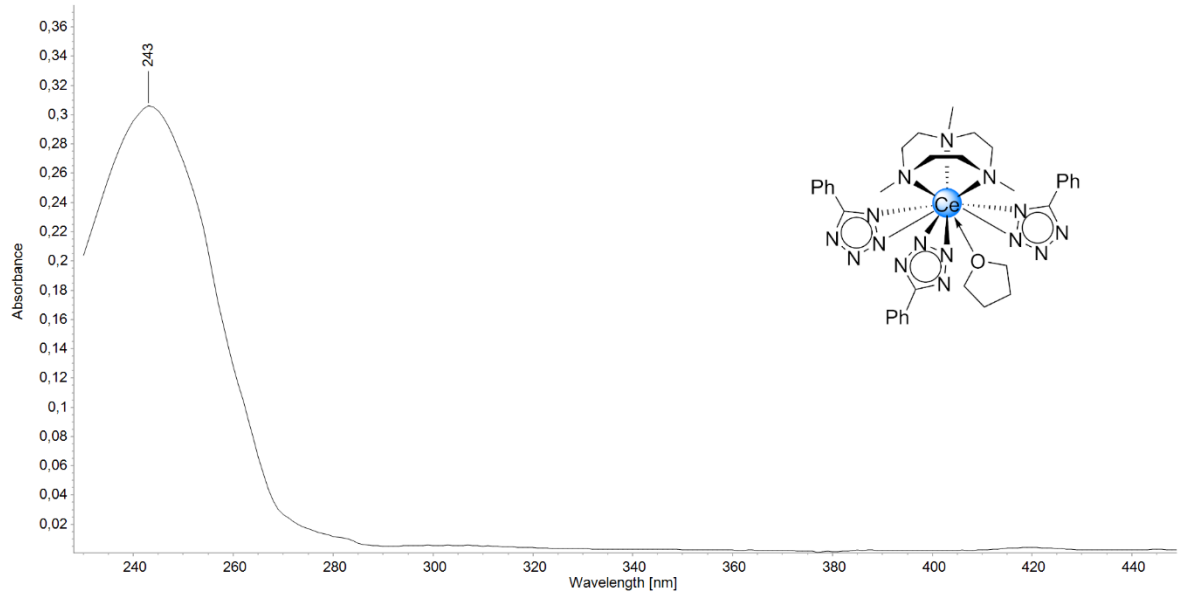

Figure S43. Absorption spectrum of a 10 µM solution of $(Me_3TACN)Ce(tet^{Ph})_3(thf)$ (**7**) in THF.

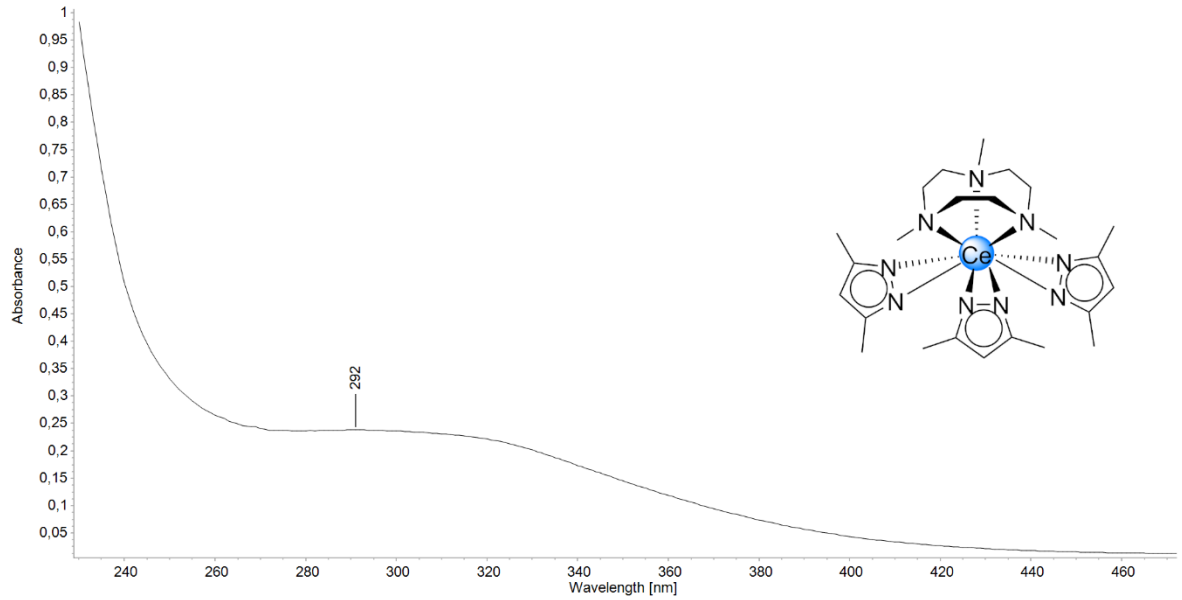

Figure S44. Absorption spectrum of a 20 µM solution of $(Me_3TACN)Ce(pz^{Me,Me})_3$ (**8**) in THF.